

Gasification of Meat and Bone Meal

A Thesis Submitted to the College of Graduate Studies and Research
in partial fulfillment of the requirements for the degree of

Master of Science

in the Department of Chemical Engineering

University of Saskatchewan

Saskatoon, Saskatchewan

By

Chirayu G. Soni

**Copyright Chirayu G. Soni, September 2009
All Rights Reserved**

COPYRIGHT

The author has agreed that the Libraries of the University of Saskatchewan make this thesis freely available for inspection. Moreover, the author has agreed that permission for copying of this thesis in any manner, either whole or in part, for scholarly purposes can be granted primarily by the professor(s) who supervised this thesis or, in their absence, by the Head of the Department of Chemical Engineering or the Dean of the College of Graduate Studies. Duplication or publication or any use of this thesis, in part or in whole, for financial gain without prior written approval by the University of Saskatchewan is prohibited. It is also understood that due recognition shall be given to the author of this thesis and to the University of Saskatchewan in any use of the material therein.

Request for the permission to copy or make any other use of the material in this thesis, in whole or in part, should be addressed to:

The Head
Department of Chemical Engineering
College of Engineering
University of Saskatchewan
57 Campus Drive
Saskatoon, Saskatchewan, Canada
S7N 5A9

ABSTRACT

Meat and bone meal (MBM) is a byproduct of the rendering industries. It is found to be responsible for the transmission of bovine spongiform encephalopathy (BSE) in animals and is no longer used as a feed to animals. There are various methods for disposal of MBM such as land filling, incineration, combustion, pyrolysis and gasification. Gasification appears to be one of the best options. High temperature of gasification reaction destroys the potential BSE pathogens and produces gases which can be further used to produce valuable liquid chemicals by Fischer-Tropsch synthesis or to generate electricity. Gasification of meat and bone meal followed by thermal cracking/ reforming of tar was carried out using oxygen and steam separately at atmospheric pressure using a two-stage fixed bed reaction system in series. The first stage was used for the gasification and the second stage was used for thermal cracking/ reforming of tar.

Meat and bone meal was successfully gasified in the two-stage fixed bed reaction system using two different oxidants (oxygen and steam) separately. In gasification using oxygen, the effects of temperature (650 – 850 °C) of both stages, equivalence ratio (ER) (actual O₂ supply/stoichiometric O₂ required for complete combustion) (0.15 – 0.3) and the second stage packed bed height (40 – 100 mm) on the product (char, tar and gas) yield and gas (H₂, CO, CO₂, CH₄, C₂H₄, C₂H₆, C₃H₆, C₃H₈) composition were studied. It was observed that the two-stage process increased hydrogen production from 7.3 to 22.3 vol. % (N₂ free basis) and gas yield from 30.8 to 54.6 wt. % compared to single stage. Temperature and equivalence ratio had significant effects on the hydrogen production and product distribution. It was observed that higher gasification (850 °C) and cracking (850°C) reaction temperatures were favorable for higher gas yield of 52.2 wt. % at packed bed height of 60 mm and

equivalence ratio of 0.2. The tar yield decreased from 18.6 wt. % to 14.2 wt. % and that of gas increased from 50.6 wt. % to 54.6 wt. % by changing the packed bed height of second stage from 40 to 100 mm while the gross heating value (GHV) of the product gas remained almost constant (16.2 – 16.5 MJ/m³).

In gasification using steam, effects of temperature (650 – 850 °C) of each stage, steam/MBM (wt/ wt) (0.4 -0.8), and packed bed height (40 -100 mm) in second stage on the product (Char, liquid and gas) distribution and gas (H₂, CO, CO₂, CH₄, C₂H₄, other H/C) composition were studied. It was observed that higher reaction temperature (850 °C) was favorable for high gas and hydrogen yields. Char gasification improved from 27 to 13 wt. % and hydrogen yield increased from 36.2 to 49.2 vol. % with increase in steam/MBM (wt/ wt), while with increased in packed bed height increased gas (29.5 to 31.6 wt. %) and hydrogen (45 to 49.2 vol. %) yields. It didn't show substantial effect on heavier hydrocarbons.

The kinetic parameters for the pyrolysis of meat and bone meal were determined using thermogravimetric analysis (TGA) at three different heating rates (10, 15 and 25 °C/min) using distributed activation energy model (DAEM). The activation energy was found in the range of 60-246 kJ/mol for the temperature range of 496-758 K and their corresponding frequency factors were 6.63×10^3 to $8.7 \times 10^{14} \text{ s}^{-1}$.

ACKNOWLEDGEMENTS

I wish to express my appreciation to my supervisors, Drs. Ajay Dalai and Todd Pugsley, and my advisory committee member, Dr. Terry Fonstad, whose guidance throughout my program facilitated me to the success of this research work. Discussion with Dr. Zhiguo Wang during weekly/ bi-weekly meetings is also appreciated. I am grateful to Dr. C. Niu including all other committee members for their valuable suggestions and comments during the committee meetings. Special thanks to Drs. Ajay Dalai and Todd Pugsley for giving their feedback on my reports, manuscript, and thesis draft which helped me sharpen my writing skills.

I would like to thank T. Wallentiny, R. Blondin, and D. Cekic of the Chemical Engineering Department for their technical assistance for various stages of this work. My sincere thanks to T. Wallentiny and R. Blondin without whom I could not repair the gas chromatographs.

I am also thankful to all members of the Catalysis and Reaction Engineering Lab for their kind co-operation through out my program. I must appreciate the financial support from TSE research fund and Agricultural Development Fund for this research work.

Last but not the least, I greatly appreciate support from my parents, other family members, and friends.

DEDICATION

I dedicate this work to

My parents, Grand parents, Sister, and

Every moment I've spent

TABLE OF CONTENTS

	Page
COPYRIGHT	i
ABSTRACT	ii
ACKNOWLEDGEMENTS	iv
DEDICATION	v
TABLE OF CONTENTS	vi
LIST OF TABLES	ix
LIST OF FIGURES	xi
NOMENCLATURE	xv
1. INTRODUCTION	1
1.1 Different options to dispose Meat and bone meal	1
1.1.1 Incineration/ Co-incineration	2
1.1.2 Land-filling and alkaline hydrolysis	2
1.1.3 Novel treatments: pyrolysis, gasification, and combustion	3
1.2 Knowledge gap	5
1.3 Objectives	5
2. LITERATURE REVIEW	7
2.1 Background	7
2.2 Biomass Gasification	10
2.2.1 Biomass gasification using oxygen/ air	13
2.2.2 Biomass gasification using steam	17
2.3 Kinetic analysis for pyrolysis of meat and bone meal	20

3. EXPERIMENTAL	24
3.1 System description	24
3.1.1 Phase I: Gasification of Meat and Bone Meal Using Oxygen	24
3.1.2 Phase II: Gasification of Meat and Bone Meal Using Steam	26
3.2 Experimental procedure	28
3.2.1 Phase I: Gasification of Meat and Bone Meal Using Oxygen	28
3.2.2 Phase II: Gasification of Meat and Bone Meal Using Steam	29
3.2.3 Phase III: Pyrolysis of Meat and Bone Meal in a Thermogravimetric Analyzer	30
3.3 Analysis of meat and bone meal, inert packed bed material, and product gases	30
3.4 Experimental design	31
4. RESULTS AND DISCUSSION	33
4.1 Particle size distribution, proximate and ultimate analysis of meat and bone meal	33
4.2 Gasification of meat and bone meal using oxygen	36
4.2.1 Single stage operation	36
4.2.1.1 Effect of temperature	36
4.2.2 Two-stage operation	38
4.2.2.1 Effect of temperature	38
4.2.2.2 Effect of equivalence ratio	40
4.2.2.3 Effect of packed bed height	42

4.3	Gasification of meat and bone meal using steam	45
4.3.1	Single stage operation	45
4.3.1.1	Effect of temperature	45
4.3.2	Two-stage operation	47
4.3.2.1	Effect of temperature	47
4.3.2.2	Effect of steam/MBM ratio	49
4.3.2.3	Effect of packed bed height	51
4.4	Comparison of phase I and II results	53
4.4.1	Single-stage operation	53
4.4.2	Two-stage operation	53
4.5	Determination of kinetic parameters using distributed activation energy model	55
4.5.1	Introduction	55
4.5.2	Results and discussion	56
5.	CONCLUSIONS AND RECOMMENDATIONS	61
6.	REFERENCES	65
	APPENDIX A: Calibration of mass flow meters, syringe pump, and GCs HP 5880 and 5890	73
	APPENDIX B: Sample calculation for mass balance and calorific value of product gas	79
	APPENDIX C: Experimental results with replicate runs	82
	APPENDIX D: Permissions for figures and tables	94

LIST OF TABLES

Table		Page
Table 2.1	Projection of energy use by fuel type	8
Table 2.2	Biomass potential and use distribution between regions, 10 ³ PJ/year [Skytte <i>et al.</i> , 2006]	11
Table 2.3	Possible reactions for gasification coal or biomass	13
Table 2.4	Effect of key parameters on product distribution and gas composition for air/ oxygen blown gasification	16
Table 2.5	Effect of key parameters on product distribution and gas composition for the steam gasification of biomass	20
Table 3.1	Experimental plan	32
Table 4.1	Proximate and ultimate analysis of meat and bone meal	35
Table B1	Calculation for gas compositions and weight of product gas	80
Table B2	Calculation for calorific value of product gas	81
Table C1	Effect of temperature during single-stage operation	82
Table C2	Effect of temperature during two-stage operation	83
Table C3	Effect of equivalence ration in two-stage operation	84
Table C4	Effect of packed bed height during two-stage operation	85
Table C5	Replicate runs of Phase I	86
Table C6	Effect of temperature during single stage operation	88
Table C7	Effect of temperature during two-stage operation	89
Table C8	Effect of steam/MBM during two-stage operation	90
Table C9	Effect of packed bed height during two-stage operation	91

LIST OF FIGURES

Figure		Page
Fig. 2.1	World marketed energy consumption, 1980-2030	7
Fig. 2.2	Shares of world's primary energy consumption [Han and Kim, 2006]	8
Fig. 2.3	Historical and future CO ₂ emissions by countries/ regions [Timilsina, 2008]	9
Fig. 2.4	Reaction sequence for gasification of coal or biomass	12
Fig. 3.1	Schematic diagram of experimental setup for gasification of meat and bone meal using oxygen in two-stage fixed bed reaction system	25
Fig. 3.2	Schematic diagram of experimental setup for steam gasification of meat and bone meal in two-stage fixed bed reaction system	27
Fig. 4.1	Particle size distributions of (a) Ottawa sand and (b) MBM powder	34
Fig. 4.2	Effect of first stage final temperature on product yield and GHV of gas at ER of 0.2 and N ₂ flow rate of 45 ml/min	37
Fig. 4.3	Effect of final temperature of first stage on gas composition at ER of 0.2 and N ₂ flow rate of 45 ml/min	37
Fig. 4.4	Effect of second stage temperature on product yield and GHV of gas at first stage final temperature of 850 °C, ER of 0.2, N ₂ flow rate of 45 ml/min and packed bed height of 60 mm	39
Fig. 4.5	Effect of second stage temperature on gas composition at first stage final temperature of 850 °C, ER of 0.2, N ₂ flow rate of 45 ml/min and packed bed height of 60 mm	39

Fig. 4.6	Effect of equivalence ratio (ER) on product yield and GHV of gas at first stage final and second stage temperatures of 850 °C and packed bed height of 60 mm	41
Fig. 4.7	Effect of equivalence ratio (ER) on gas composition at first stage final and second stage temperatures of 850 °C and packed bed height of 60 mm	41
Fig. 4.8	Effect of packed bed height on product yield at first stage final and second stage temperatures of 850 °C, ER of 0.2 and N ₂ flow rate of 45 ml/min	43
Fig. 4.9	Effect of packed bed height on gas compositions at first stage final and second stage temperatures of 850 °C, ER of 0.2 and N ₂ flow rate of 45 ml/min	43
Fig. 4.10	Effect of final temperature of first stage on product yield at steam/MBM (wt. /wt.) of 0.6 and N ₂ flow rate of 45 ml/min	46
Fig. 4.11	Effect of final temperature of first stage on gas composition at steam/MBM (wt. /wt.) of 0.6 and N ₂ flow rate of 45 ml/min	46
Fig. 4.12	Effect of second stage temperature on product yield at first stage final temperature of 850 °C, steam/MBM (wt. /wt.) of 0.6, N ₂ flow rate of 45 ml/min and packed bed height of 60 mm	48
Fig. 4.13	Effect of second stage temperature on gas composition at first stage final temperature of 850 °C, steam/MBM (wt. /wt.) of 0.6, N ₂ flow rate of 45 ml/min and packed bed height of 60 mm	48

Fig. 4.14	Effect of steam/ MBM (wt/ wt) on product yield at final temperature of first stage and second stage at 850 °C, N ₂ flow rate of 45 ml/min and packed bed height of 60 mm	50
Fig. 4.15	Effect of steam/ MBM (wt/ wt) on gas composition at final temperature of first stage and second stage at 850 °C, N ₂ flow rate of 45 ml/min and packed bed height of 60 mm	50
Fig. 4.16	Effect of packed bed height on product yield at steam/ MBM (wt/ wt) of 0.8, final temperature of first stage and second stage at 850 °C, and N ₂ flow rate of 45 ml/min	52
Fig. 4.17	Effect of packed bed height on gas composition at steam/ MBM (wt/ wt) of 0.8, final temperature of first stage and second stage at 850 °C, and N ₂ flow rate of 45 ml/min	52
Fig. 4.18	Comparison of phase I and II results during single stage operation	54
Fig. 4.19	Comparison of phase I and II results during two - stage operation	54
Fig. 4.20	Effect of temperature on V/V* during pyrolysis of MBM in thermogravimetric analyzer for three different heating rates	58
Fig. 4.21	$\ln(a/T^2)$ vs. $1/T$ at the selected V/V* ratios	58
Fig. 4.22	V/V* vs. E relationship	59
Fig. 4.23	$\ln k_0$ vs. E relationship	59
Fig. 4.24	$f(E)$ vs. E relationship	60
Fig. A.1	Calibration of mass flow meter (0-200 ml/min)	73
Fig. A.2	Calibration of mass flow meter (0-20 ml/min)	74

Fig. A.3	Calibration of mass flow meter	74
Fig. A.4	Calibration curve of H ₂	75
Fig. A.5	Calibration curve of CO	75
Fig. A.6	Calibration curve of CO ₂	76
Fig. A.7	Calibration curve of CH ₄	76
Fig. A.8	Calibration curve of C ₂ H ₄	77
Fig. A.9	Calibration curve of C ₂ H ₆	77
Fig. A.10	Calibration curve of C ₃ H ₆	78
Fig. A.11	Calibration curve of C ₃ H ₈	78

NOMENCLATURE

F_i	fraction i of the sample to decompose,
V_i	volatiles produced by fraction i
S_i	solid residue formed.
w_i	weight fraction (actual weight/initial weight) for fraction i
k_{i0}	pre-exponential factor (s^{-1} mass fraction $^{1-n_i}$)
E_i	activation energy ($kJ\ mol^{-1}$)
n_i	reaction order
R	gas constant ($kJ\ mol^{-1}\ K$)
T	temperature (K)
$w_{i\infty}$	weight fraction at time infinity that accounts for the final residue of the process
V	total volatiles evolved by time t
V^*	effective volatile content
a	heating rate (K/min)
$f(E)$	distribution curve of the activation energy
LHV	lower heating value
ER	equivalence ratio
DSS	dry sewage sludge
u_{mf}	minimum fluidization velocity
TDE	transmissible degenerative encephalopathies

Chapter 1

INTRODUCTION

1.1 Different options to dispose Meat and bone meal

Meat and bone meal or MBM is a byproduct of the rendering industries. It is obtained after removal of fat from mammal carcasses during the cooking process followed by drying and crushing [Bradley, 1991]. MBM has historically been used worldwide in the formulation of feed for cattle because of its high protein content, but after being found to be responsible for the spreading of bovine spongiform encephalopathy (BSE), its use has become progressively restricted [Rodehutschord *et al.*, 2002]. The European Commission has banned the use of protein derived from mammalian tissues for feeding ruminants since July 1994 [Chalus and Peutz, 2000]. Moreover, the link between BSE and new variant of “creutzfeldt-Jacob disease (vCJD)” in humans has made MBM a critical issue [Bruce *et al.*, 1997].

MBM is produced in large amounts and requires a safe disposal method to avoid the spreading of BSE. In United States around 2.1 millions metric tons of bovine, porcine, or mixed species of MBM was produced in 2004, while in Canada, it was 432,000 metric tons in 2000 [Garcia *et al.*, 2006]. The current production of MBM in the EU is approximately 3 millions tons per year [<http://ec.europa.eu>].

Since these large volume of meat and bone meal can no longer be used as a feed to animals, alternative safe disposal methods to avoid spreading of bovine spongiform encephalopathy are required. The following sections outline various methods for disposal of meat and bone meal.

1.1.1 Incineration/ Co-incineration

It has been reported that the responsible prions for BSE pathogens are destroyed by combustion at 850 °C for at least 2 sec, or at 3 bar and 133 °C for at least 20 min [Ayllon *et al.*, 2006]. Incineration/ co-incineration is the potential solution for safe disposal of meat and bone meal. The high incinerator temperature ensures complete destruction of prions responsible for bovine spongiform encephalopathy. There are various incineration plants in England and Belgium for incineration of meat and bone meal and they are operated when there is an assurance of sufficient supply of meat and bone meal [Conesa *et al.*, 2003]. An issue with this method is the ash handling. The ash tends to stick on the bottom of the incinerator chamber causing problem in a continuous operation.

Meat and bone meal can also be disposed of by co-incineration in cement kilns. The high temperature of the cement kiln (around 1400 - 1450 °C) and sufficient residence time ensure complete destruction of potential BSE pathogens [Cyr and Ludmann, 2006]. In the US, there are around 30 separate sites where hazardous waste is burned in cement kilns [Conesa *et al.*, 2003].

1.1.2 Land-filling and alkaline hydrolysis

Land-filling was one of the options considered. It was ruled out due to high risk of spreading potential BSE pathogens into the environment. However, a research work by Gulyurtlu *et al.* [2005] concluded that the solid products (i.e. ashes) of a thermally pre-treated meat and bone meal could be safely deposited in landfills. The authors reported that ashes obtained after co-combustion of meat and bone meal with coal at relatively low

temperatures (750 - 850 °C) were free from harmful proteins and safe in normal municipal landfills.

Inactivation of BSE prions by alkaline hydrolysis is also one of the options researchers have been working on to safely dispose meat and bone meal. Taylor *et al.* [1997] subjected samples of macerated mouse-brain infected with the 22A strain of scrapie agent to gravity-displacement autoclaving at 121 °C for 30 min in the presence of 2 M sodium hydroxide and found no infectivity in mouse bioassay. They concluded the similar treatment could be effective for human and animal TSE agents.

1.1.3 Novel treatments: pyrolysis, gasification, and combustion

Apart from the above methods, combustion, pyrolysis and gasification are other methods for disposal of meat and bone meal at elevated temperature for complete destruction of potential BSE pathogens and effectively utilize the fuel value. The main difference among these methods is the amount of oxygen supply. Combustion requires oxygen in excess of that required to theoretically burn the feed material and mainly produces carbon dioxide and water along with heat. Pyrolysis is the thermal conversion of organics in the absence of oxygen supply and mainly produces liquid products, called pyrolytic oil or tar. Gasification requires controlled/ partial oxygen supply and mainly produces gases containing carbon monoxide and hydrogen (CO + H₂), a mixture known as syngas. The following discussion presents a brief summary of research studies carried out on meat and bone meal pertaining to this section.

Ayllon et al. [2006] studied the effect of final pyrolysis temperature (300-900 °C) and heating rate (2, 8 and 14 °C /min) on the fixed bed pyrolysis of MBM. Char and tar were the

main products with relatively small amount of gas. The product gas mainly consisted of CO₂, CO, H₂, CH₄, other H/C, and H₂S. The lower heating value of product gas increased to 16.7 MJ/m³ with temperature until 500 °C and then decreased to 12.5 MJ/m³ at temperature higher than 600 °C. The authors also concluded that the final pyrolysis temperature was more important than the effect of heating rate. Chaala and Roy [2003] studied vacuum pyrolysis of MBM at a temperature of 500 °C with total pressure of 4 kPa and heating rate of 15 °C /min. They found that pyrolytic oil and solid residue were the main products with small amount of gases. The pyrolytic oil obtained was highly viscous and waxy in nature with very unpleasant odor. The high calorific value of this oil was found to be 34.2 MJ/kg. However, high nitrogen content (14 wt. %) was the main concern addressed by the authors for use of this oil in the combustion process. *Fedorowicz et al.* [2007] studied the gasification of feed consisting of MBM, cow carcasses, and two types of specific risk materials (SRMs) at 1000 °C with steam and nitrogen as carrier gases in a bench scale gasification system. The product gas mainly consisted H₂, CO, CO₂, CH₄, other H/C gases. The heating value of the product gas on nitrogen free basis was in the range from 14.9 to 19.4 MJ/m³. A major issue encountered by the authors was the production and handling of tar. Other studies include: fluidized bed co-combustion of MBM with coals and olive bagasse [Fryda *et al.*, 2006], co-combustion of coal and MBM in a fluidized bed [Gulyurtlu *et al.*, 2005], and the use of atmospheric bubbling fluidized bed combustor for the utilization of raw animal wastes [Pilawska *et al.*, 2004]. The main issue associated with co-combustion was the emissions of NO_x, VOC, and other gases harmful to the environment. Other issues related to palletizing and limiting the amount of MBM fed along with co-combustion material were also mentioned by the authors.

1.2 Knowledge gap

Literature review on meat and bone meal reveals that research has been done on pyrolysis, combustion/ co-combustion and gasification of meat and bone meal. So far there is no scientific investigation done to increase the hydrogen and syngas yield via gasification of meat and bone meal in a fixed-bed reactor system followed by thermal cracking of tar using oxygen/air and steam separately.

1.3 Objectives

The overall objective of this research work is to gasify meat and bone meal and maximize the production of hydrogen and syngas in single stage and two-stage fixed reactor systems. The research was carried out in three different phases as follows:

Phase I: In this phase, the gasification of MBM was carried out in single stage and two-stage reactor systems. Pure oxygen was used as a gasifying agent and nitrogen was used as a carrier gas. The first stage was used for gasification while the second one was used to facilitate tar cracking to produce further gases. The effects of temperature of each stage (650-850 °C), equivalence ratio (0.15-0.3), and packed bed height (40-100 mm) were studied on product yields (char, tar, and gas) and gas compositions (H_2 , CO, CO_2 , CH_4 and other H/C).

Phase II: In this phase, the gasification of MBM was carried out in single stage and two-stage reactor systems using steam as a gasifying agent and nitrogen as a carrier gas. The effects of temperature of each stage (650-850 °C), steam to meat and bone meal ratio (0.2-0.8) (wt/ wt), and packed bed height (40-100 mm) were studied on product yields (char, tar, and gas) and gas compositions (H_2 , CO, CO_2 , CH_4 and other H/C).

Phase III: Pyrolysis or devolatilization is a very important step in the gasification process. It is very complex and involves number of series and/ or parallel reactions occurring simultaneously. In this phase, the kinetic analysis for pyrolysis of MBM was carried out using thermogravimetric analysis (TGA) at three different heating rates (10, 15, and 25 °C/min) for the temperature range of 25-550 °C. The simple distributed activation energy model (DAEM) developed by Miura and Maki [1998] was used to determine activation energy, E , and frequency factor, k_0 .

Chapter 2

LITERATURE REVIEW

2.1 Background

World energy demand increases day by day. According to EIA [2009], the total world energy consumption in 2006 was 472 quadrillion BTU. This is projected to increase to 678 quadrillion BTU by 2030, as shown in Fig. 2.1. This rise in energy consumption is almost 44 % and is mainly due to China and India emerging as the fastest growing economies in the world.

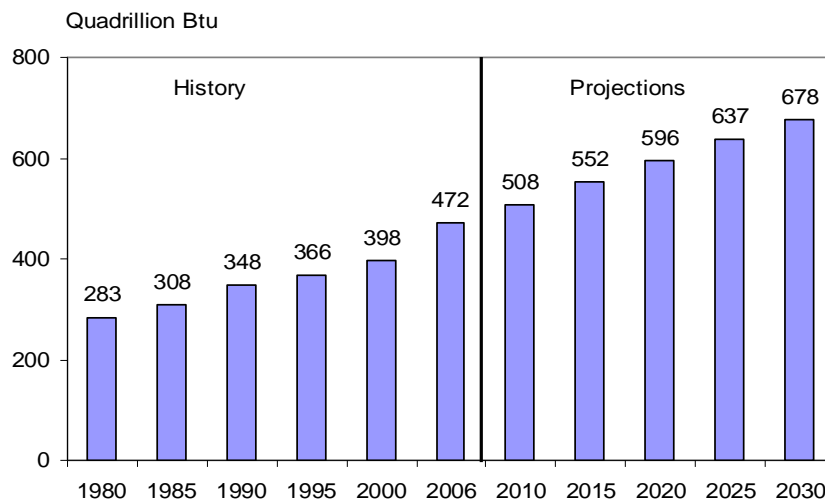


Fig. 2.1 World marketed energy consumption, 1980-2030
[Reproduced from EIA, 2009; 1 BTU international = 0.001055 MJ]

Most of the world's energy demand is met by fossil fuels and the technologies for them are very well established. Various non-renewable sources of energy such as coal, crude oil, natural gas etc. have been exploited over the years to meet energy demand of the world. Fig. 2.2 shows the distribution of energy consumption based on the fuel type [Han and Kim, 2006]. As seen in this figure, oil, natural gas, and coal contribute nearly 73 % of the total demand, while the rest include renewable sources, nuclear etc. The projection of energy use

by fuel types is shown in Table 2.1 [EIA, 2009]. It is clear that the use of coal and unconventional resources, compared to other fuel types, is going to increase the most in the coming years to help meet the energy demand. The use of coal is going to increase from 127 quadrillion Btu in year 2006 to 190 quadrillion Btu in year 2030, while that of unconventional resources of liquid fuel are going to increase from 3.1 million barrels/ day in year 2006 to 13.4 million barrels/ day in year 2030.

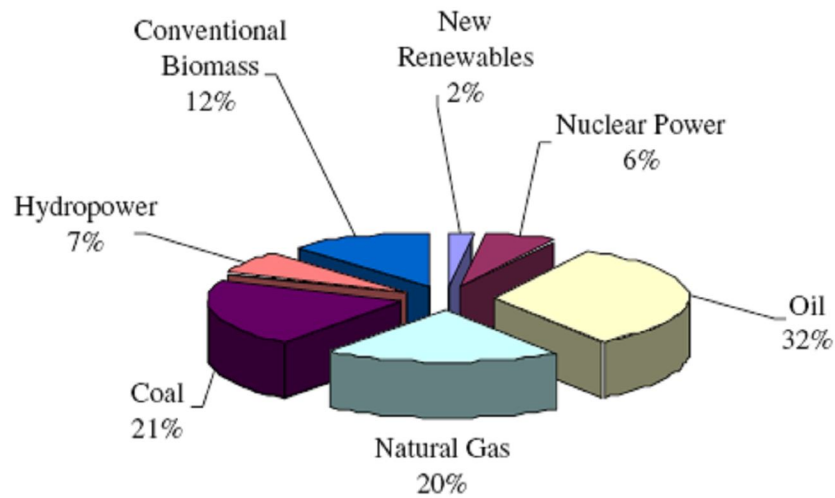


Fig. 2.2 Shares of world's primary energy consumption [Han and Kim, 2006, Used with permission]

Table 2.1 Projection of energy use by fuel type [Data source, EIA 2009]

Fuel type	Current use (2006)	Projected use (2030)
Liquid and other petroleum	85 million barrels/ day	107 million barrels/ day
Unconventional resources (including oil sands, heavy oil, bio-fuels, coal to liquid, gas to liquid)	3.1 million barrels/ day	13.4 million barrels/ day
Natural gas	104 trillion cubic feet	153 trillion cubic feet
Coal	127 quadrillion Btu	190 quadrillion Btu
Electricity from nuclear power	2.7 trillion KWhrs	3.8 trillion KWhrs

There are several disadvantages associated with the use of fossil fuels as energy sources. Environmental issues, prices, and limitation of resources are the key ones. Crude oil prices have been fluctuating frequently in recent years, sparking concerns in most of the developing and oil importing countries. Oil prices reached US \$145 per barrel in 2008 and dropped down below US \$ 40 per barrel in the next few months. Moreover, fossil fuels have caused serious environmental problems and disturbed the ecological cycle of the planet. One of the best is the green house effect, which is a major problem the world is presently facing. It is causing the average global temperature to rise, sea levels to rise due to melting of icebergs, and so forth. Fig. 2.3 shows the historical and future CO₂ emissions by countries [Timilsina, 2008]. This figure shows that the total CO₂ emissions in 1980 was 18 billion tonnes, rising to 27 billions tonnes in 2004; an increase of 50 %. The figure also predicts that in 2030, CO₂ emissions will be approximately 43 billions tonnes, and fast developing nations such as China, India along with other Asian countries will be the key contributors.

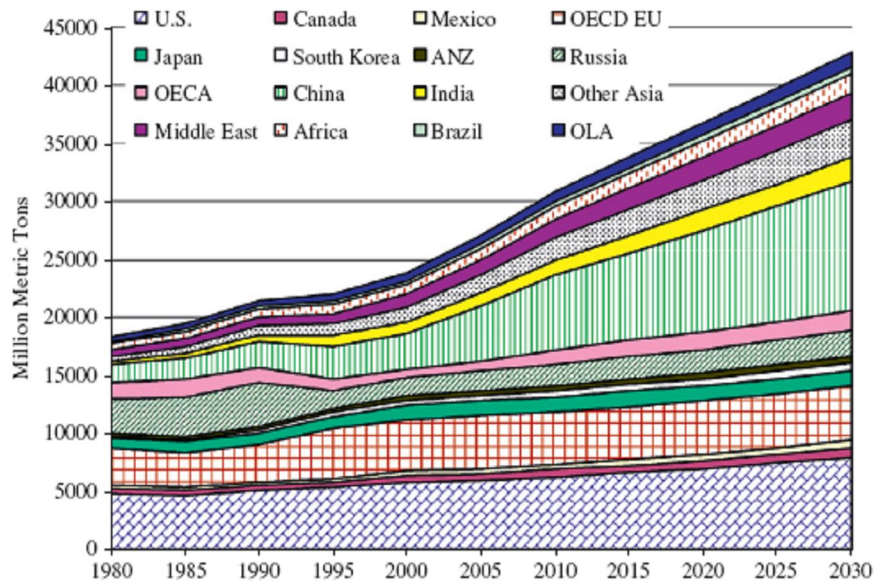


Fig. 2.3 Historical and future CO₂ emissions by countries/ regions [Timilsina, 2008, Used with permission]

Scientific speculations on depletion of fossil fuels encourage researchers from across the world to find alternative form of energy. Nuclear energy is one of the viable alternatives, however, capital cost, broad policy acceptance, and nuclear waste management challenges are associated with this option. Another promising option is biomass energy. Some important facts why biomass energy is drawing attention are [Demirbas *et al.*, 2009]:

1. It meets energy needs without expensive conversion devices
2. It is carbon neutral
3. It can deliver energy in all forms that people need
4. It helps to restore unproductive and degraded lands, soil fertility and water retention
5. It contributes to poverty reduction in developing nations

2.2 Biomass Gasification

There are various sources of biomass such as wood and wood wastes, agricultural crops and their wastes, animal wastes, waste from food processing etc. Presently, the available biomass resources could provide as much as $6.33 - 10.55 \times 10^{12}$ MJ of feed-stock energy [Demirbas *et al.*, 2009]. Table 2.2 [Skytte *et al.*, 2006] shows that Asia, Latin America and Africa have the highest biomass potential. From the table, Asia uses more biomass than the actual annual potential while former USSR, Middle East and Latin America use less than the actual potential. Biomass mainly contains carbon, hydrogen, oxygen, nitrogen, and sulfur along with other heavy metals in small amounts. The high heating value of biomass varies from source to source. It is in the range of 10 to 20 MJ/ kg which is

comparable to the high heating value of coal (15 - 33 MJ/kg) [Channiwala and Parikh, 2002; Perry and Green, 1997].

Table 2.2 Biomass potential and use distribution between regions, 10^3 PJ/year (1 PJ= 10^{15} J) [Skytte *et al.*, 2006, Used with permission]

Biomass potential	North America	Latin America	Asia	Africa	Europe	Middle East	Former USSR	World
Wood biomass	12.8	5.9	7.7	5.4	4	0.4	5.4	41.6
Energy crops	4.1	12.1	1.1	13.9	2.6	0	3.6	37.4
Straw	2.2	1.7	9.9	0.9	1.6	0.2	0.7	17.2
Other	0.8	1.8	2.9	1.2	0.7	0.1	0.3	7.6
Total potential	19.9	21.5	21.6	21.4	8.9	0.7	10	103.8
Use	3.1	2.6	23.2	8.3	2	0	0.5	39.7
Use/ potential (%)	16	12	107	39	22	7	5	38

There are three main routes for the conversion of biomass to useful energy: biochemical, chemical, and thermochemical. The focus of the present study is Thermochemical. Thermochemical processes such as pyrolysis, gasification and combustion have received special attention since they yield useful products and simultaneously contributes to solving problems arising from biomass accumulation [Della Rocca *et al.*, 1999]. Combustion is a thermochemical oxidation process in which excess oxidant (typically O_2 in air) is supplied. This process is mainly used to generate heat and electric power. Pyrolysis is carried out in the absence of oxygen and mainly produces high heating value pyrolytic oil. Gasification can be described as the thermochemical conversion of carbonaceous feed stock into gaseous products by supplying heat and a controlled or limited amount of oxygen that is less than that theoretically needed for complete combustion. The gases produced mainly contain syngas ($CO + H_2$) along with methane and other hydrocarbons in small amounts. These product gases could be used either to produce electricity or valuable chemicals such as methanol, dimethylether, alcohols etc. via Fischer-Tropsch synthesis [Han and Kim, 2006]. The overall gasification process involves pyrolysis/

devolatilization which produces char followed by gasification of char to produce gaseous products as shown in Fig. 2.4 [Higman and Van der Burgt, 2008].

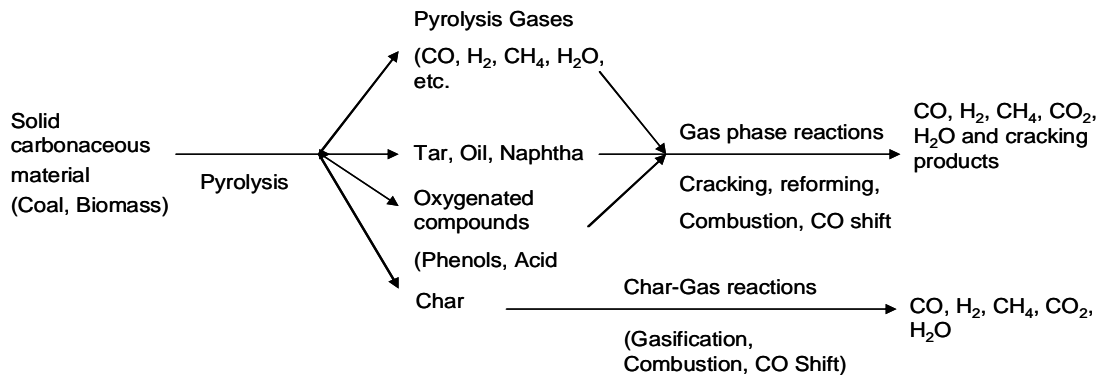


Fig. 2.4 Reaction sequence for gasification of coal or biomass (Reproduced from Higman and Van der Burgt, 2008)

As per the reaction scheme, the initial step in coal or biomass gasification is pyrolysis, which produces a variety of species (tars, hydrocarbons liquids, pyrolysis gases such as CH_4 , CO , H_2 , H_2O , and char). In the second step, two different types of reactions take place: gas phase reactions (cracking, reforming, combustion, shift reaction) and char-gas reactions (gasification, combustion, etc.). The summary of possible reactions is presented in Table 2.3 [Higman and Van der Burgt, 2008]. Combustion, methanation and CO-shift reactions are exothermic while Boudouard, water gas and reforming reactions are endothermic. When the system is in thermal balance, the heat evolved through exothermic reactions is utilized by endothermic reactions. The partial combustion reaction of char and Boudouard reactions are important for the production of pure CO, while the CO-shift reaction is the deciding factor for CO and CO_2 ratio in product gases.

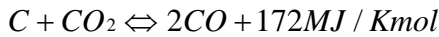
Biomass may be gasified by using pure oxygen, air, steam or combination of these with or without the use of a catalyst. The following section reviews biomass gasification using oxygen/ air and steam.

Table 2.3 Possible reactions for gasification of coal or biomass

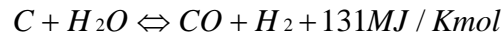
Combustion reactions



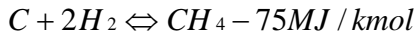
Boudouard reaction



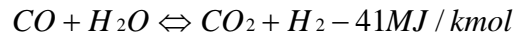
Water gas reaction



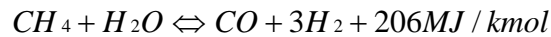
Methanation reaction



CO shift reaction



Steam methane reforming reaction



2.2.1 Biomass gasification using oxygen/ air

Many researchers have used oxygen/air as a source of oxidant in the gasification process. Use of pure oxygen gives accurate control of oxygen supply to the reaction and at the same time the effect of gas residence time on product yield can also be studied by varying the inert gas flow rate. The following discussion focuses on a few important studies carried out on biomass gasification using oxygen/ air.

Xiao et al. [2007] studied the effect of equivalence ratio (ER), bed height and fluidization velocity ratio (u/u_{mf}) on gasification of polypropylene plastic waste in a fluidized

bed gasifier using air pre-heated to 400 °C. They observed that with increase in ER from 0.2 to 0.45, gas yield increased from 76.1 to 94.4 wt. %, while tar and char yield decreased to almost negligible at 15.9 to 5 wt. % respectively keeping other parameters constant. H₂ and CO yields first increased with ER to a maximum yield and then decreased. The increase in CO and H₂ yields is due to thermal cracking of tar at higher temperature, which is consistent with the decrease in tar production and C₂₊. While changing the static bed height from 100 to 300 mm, they found enhancement in secondary cracking reactions of tar and heavy hydrocarbons and char gasification as well. The H₂ content was almost constant, while methane and other hydrocarbons decreased slightly with increase in static bed height. The CO and CO₂ contents reached maximum values for the static bed height of 200 mm. With increase in fluidization velocity ratio (u/u_{mf}) from 2 to 4, the char yield was increased from 9 to 12 wt. % as the ratio increased from 3 to 4, while on the other hand, the gas yield was decreased from 87.5 to 85 wt. % and that of tar decreased slightly as well. With increasing the ratio u/u_{mf} from 2 to 4, CO, H₂ and C_nH_m decreased from 22.7 to 18.9 %, from 5.7 to 4.9 % and from 3.9 to 3.5 % respectively.

Narvaez et al. [1996] studied biomass air gasification in a bubbling fluidized bed gasifier using calcined dolomite catalyst in the guard bed reactor. They found that with increase in equivalence ratio (ER) from 0.2 to 0.45 for gasifier temperature at 800 °C, freeboard temperature at 600 °C, and H/C (fed to the gasifier) at 2.3, the amount of fuel gases (H₂, CO, CH₄, and C₂H₂), and tar yield in the gas decreased, while gas yield increased. Maximum H₂ yield was obtained at an ER of 0.26. They observed that upon increasing the gasifier bed temperature from 700 to 850 °C keeping ER at 0.3, and H/C at 2.1, H₂ yield increased from 5 to 10 vol. %, CO yield increased from 12 to 18 vol. %, CO₂ yield

decreased with increase in temperature while no significant variation observed in CH₄ and other hydrocarbons.

Manya et al. [2006] studied the effects of bed height (100-150 mm) and equivalence ratio (air ratios: 25 %, 30 %, and 35 %) of air gasification of sewage sludge on gas yield and composition, average cold gas efficiency (defined as the ratio of the LHV of the produced gas to the LHV of the DSS fed), and raw gas tar content in a bubbling fluidized bed at 850 °C. From the statistical analysis of the data, they concluded that the influence of air ratio was more significant than the effect of bed height. They observed that with increase in air ratio from 24 to 35 %, the concentrations of H₂, CO, CH₄, C₂H₄, and C₂H₆ decreased. With an increase in bed height from 150 to 300 mm, the concentrations of the above components increased. In the case of CO₂, its percentage was not affected either by the air ratio or the bed height but only weakly for the interaction of these factors. It was also observed that concentration of C₂H₂ was affected only by the bed height and not by air ratio. The y_{gas} (specific yield to gas obtained) and y_{carbon} (average percentage of carbon in the biomass recovered in the gas) increased as equivalence ratio and bed height were increased. The LHV (lower heating value) was decreased as equivalence ratio increased while the average cold gas efficiency had no dependence on the air ratio.

Mansaray et al. [1999] studied the effects of fluidization velocity (0.22, 0.28, and 0.33 m/s) and equivalence ratio (0.25, 0.3, and 0.35) for the air gasification of rice husk in a fluidized bed gasifier. The average temperature of the dense bed varied from 665 to 828 °C depending on the operating conditions. It was observed that as equivalence ratio was increased, the concentration of CO₂ increased while the concentration of the fuel gases (CO, H₂, CH₄, C₂H₂ + C₂H₄ and C₂H₆) decreased. Increasing the fluidization velocity slightly

increased the concentration of CO₂ and decreased the concentrations of CO, H₂, CH₄, C₂H₂ + C₂H₄ and C₂H₆ which is due to the higher degree of combustion taking place at higher values of equivalence ratio and/ or fluidization velocity. The gas yield varied between 1.3 and 1.98 Nm³/ kg fuel depending on the operating conditions. An increase was observed with increasing in equivalence ratio, but not appreciably affected by the changes in the fluidization velocity. The carbon conversion varied between 55 to 81 % depending on the equivalence ratio and fluidization velocity. Carbon conversion increased with equivalence ratio due to a decrease in char formation, while increasing the fluidization velocity caused reduced the residence time of gases and enhanced carry over of fine char particles from the bed, thus decreased carbon conversion.

Based on the literature, a qualitative summary of the effect of key operating parameters on product distribution and gas composition, when using air/ oxygen blown gasification, is presented in Table 2.4.

Table 2.4 Effect of key parameters on product distribution and gas composition for air/ oxygen blown gasification

	Temperature (+)	Equivalence ratio (+)	Fluidization velocity (+)	Bed height (+)
Char conversion	+	+	-	+
Tar yield	-	-	-	-
Gas yield	+	+	-	+
H ₂ yield	+	-	-	+ (marginal)
CO yield	+	-	-	+
CO ₂ yield	-	+	+	+
CH ₄ yield	Not significant	-	Unclear	Unclear
Other H/C yield	Not significant	-	-	Unclear

+: increase, -: decrease

2.2.2 Biomass gasification using steam

Many researchers have studied biomass gasification using steam and found it beneficial for adjusting the gas composition and improving the hydrogen. The following discussion is about few important studies on steam gasification of biomass.

Franco et al. [2003] studied the steam gasification of forestry biomass in an atmospheric fluidized bed over a temperature range of 700 – 900 °C and steam/biomass ratio from 0.4 to 0.85 w/w. With an increase in temperature from 700 to 900 °C at a steam/biomass ratio of 0.8 w/w, they found an increase in gas yield and decrease in tar and char yield due to further cracking of liquids and enhanced char reaction with the gasifying medium. H₂ formation increased from 26 to 33 mol % while CO production decreased from 41 to 38 mol %. Hydrocarbon concentration decreased while there was no significant variation in CO₂ concentration, which was approximately 14 mol %. Steam/biomass ratio was varied from 0.4 to 0.85 w/w at 800 °C. It was observed that the production of gaseous products reached a maximum around steam/biomass ratio of about 0.6-0.7 w/w, which corresponded to the minimum liquid yields. H₂ formation was maximum (41 mol %) at steam/biomass ratio of 0.6 – 0.7 w/w. CO decreased with increase in ratio up to 0.6 and then remained constant. Similar trends were observed in the case of hydrocarbons as well. There was no significant variation observed in CO₂ concentration.

Wei et al. [2007] studied the effects of reaction temperature (750 - 850 °C) and steam/biomass (S/B) ratio (0.0-1.0 g/g) on product yields and the compositions of product gas in a free-fall reactor (concurrent downflow) for two different types of biomass, namely legume straw and pine sawdust. They observed that with increase in S/B ratio at 800 °C the gas yield increased while tar and char production decreased. With an increase of S/B mass

ratio from 0 to 0.6 g/g, the tar yield from legume straw decreased from 5.5 wt. % to 2.8 wt. % daf (dry ash free), while char yield decreases from 7.4 to 4.2 wt. % db (dry basis). The tar yield from pine sawdust decreases from 3.6 wt. % to 1.5 wt. % daf, while char yield decreased from 5.5 to 3 wt. % db. At higher S/B ratio from 0.8 to 1 g/g, the product yields remained constant. It was found that CO and CH₄ concentrations decreased and CO₂ and H₂ concentrations increased with an increase in S/B ratio from 0 to 0.6 g/g and at higher S/B ratio, no significant changes were detected. The H₂ concentration in the gas product from legume straw reached a maximum of 40.3 mol% at a S/B mass ratio of 0.6, while that from pine sawdust was 36.8 mol%. An increase in temperature from 750 to 850 °C at a S/B mass ratio of 0.6 g/g showed an increase in gas yield and a decrease in char and tar yield for both types of biomass. It was found that H₂ and CO₂ increased while CO and CH₄ concentration decreased with increasing reaction temperature. An H₂ concentration of 50.6 mol% and a CO concentration of 21.2 mol% were obtained from legume straw at the temperature of 850 °C, while an H₂ concentration of 44 mol% and a CO concentration of 28.2 mol% were obtained from pine sawdust.

Lv et al. [2004] studied the effects of reaction temperature (700 - 900 °C), steam to biomass (S/B) ratio (0 - 4.04), and equivalence ratio (ER) (0.19 - 0.27) on the product distribution and gas composition in air-steam gasification of pine sawdust in a fluidized bed. The gas yield and carbon conversion increased from 1.43 to 2.53 Nm³/kg biomass and 78.17 to 92.59 % respectively when reactor temperature increased from 700 to 900 °C. Equivalence ratio and S/B were held constant at 0.22 and 2.7 respectively. Regarding the gas composition, H₂ production increased while CH₄, C₂H₄, C₂H₆, and CO decreased with increasing reactor temperature. Varying the S/B ratios from 0 to 4.04 at a reactor temperature of 800 °C, and at

a equivalence ratio of 0.22, led to a carbon conversion of 92.09 % at S/B of 0.6, which then decreased to 75.19 % at the highest S/B ratio. This was reportedly the result of an excessive quantity of low temperature steam induction. It was observed that CO concentration decreased while CH₄, CO₂, and C₂H₄ concentrations increased for S/B in the range of 0 to 1.35. Over S/B range of 1.35 to 2.7, CO, CH₄ and C₂H₄ concentrations decreased, while CO₂ and H₂ concentrations increased.

Ferdous et al. [2001] studied the production of H₂ and medium heating value gas via steam gasification of lignins in a fixed-bed reactor. They studied the effect of steam flow rate (5-15 g/h/g lignin), effect of temperature (650 - 850 °C), effect of commercial steam reforming catalyst, and effect of catalyst bed temperature (600 -750 °C) on lignin conversion and product gas composition. They found that with an increasing steam flow rate from 5 to 15 g/h/g lignin, lignin conversion increased from 64 to 74 wt. % and from 74 to 85 wt. % for Alcell and Kraft lignin. Reactor temperature was held constant at 750 °C. The H₂ yield increased while that of CO and CH₄ decreased with increasing steam flow rate. This was probably due to increased char and tar reforming reactions with increasing steam flow rate. When temperature was increased from 650 to 800 °C at a steam flow rate of 5 g/h/g lignin, the lignin conversion increased from 56 to 69 wt. % and from 60 to 76 wt. % for Alcell and Kraft lignin, respectively. The concentration of H₂ and CO in the product gas increased while that of CO₂, CH₄ and C₂₊ decreased with increasing in the temperature.

Based on the literature, a qualitative summary of the effect of key parameters in steam gasification of biomass on product distribution and gas composition has been prepared (Table 2.5).

Table 2.5 Effect of key parameters on product distribution and gas composition for the steam gasification of biomass

	Temperature	Steam/ Biomass
	(+)	(+)
Char conversion	+	+
Tar yield	-	-
Gas yield	+	+
H ₂ yield	+	+
CO yield	-	-
CO ₂ yield	Unclear	Unclear
CH ₄ yield	-	Unclear
Other H/C yield	-	Unclear

+: increase, -: decrease

2.3 Kinetic analysis for pyrolysis of meat and bone meal

The pyrolysis of coal, biomass or any carbonaceous materials involves a great number of reactions. These reactions are complex and occur in parallel and series [Mansaray and Ghaly, 1999]. The design and simulation of a reactor and setting up the optimum process conditions require the knowledge of pyrolysis kinetics [Aguado *et al.*, 2002]. The most commonly used technique to study the thermal behavior of carbonaceous material is thermogravimetric analysis (TGA) [Garcia-Ibanez *et al.*, 2006]. TGA only provides general information on the overall reaction kinetics; however it could be used for providing comparative kinetic data of various reaction parameters such as temperature and heating rate. The advantage of this method is that it requires fewer data for calculating kinetic parameters than the isothermal method. The TGA method involves continuous measurement of weight loss with respect to temperature at a particular heating rate and the kinetics obtained using

this method can be examined over an entire temperature range in a continuous manner [Mansaray and Ghaly, 1999; Freeman and Carroll, 1958].

Two studies were reported in the open literature regarding thermogravimetric behavior of MBM and kinetic analysis for pyrolysis of MBM. Conesa *et al.* [2003] studied the overall kinetic parameters for the decomposition of MBM by adapting the kinetic model proposed to the temperature derivative of the weight loss of a sample under non-isothermal conditions. They carried out experiments with heating rates of 10, 20, and 30 K min⁻¹ over the temperature range of 80 to 800 °C considering three different initial fractions for the pyrolysis runs. It is as follows:



The kinetic model chosen for the analysis was a single reaction of nth order, with simplified kinetic equation as follows:

$$\frac{dw_i}{dt} = k_{i0} \exp\left(-\frac{E_i}{RT}\right)(w_i - w_{i\infty})^{n_i} \quad (2)$$

For the calculation of the total weight fraction, taking into account:

$$\sum_{i=1}^3 (w_{i0} - w_{i\infty}) = \sum_{i=1}^3 w_{i0} - \sum_{i=1}^3 w_{i\infty} = 1 - w_{\infty} \quad (3)$$

$$\text{and } w = \sum_{i=1}^3 (w_i - w_{i\infty}) + w_{\infty} \quad (4)$$

Considering an Arrhenius-type behavior of the rate constants, and considering a first-order reaction, they determined activation energies and pre-exponential constants for all fractions. The activation energies and pre-exponential factors were 30.9, 72.2, 21.5 kJ/ mol and 7.16 x 10³, 4.84 x 10⁵, 3 min⁻¹ respectively for three fractions considered. It was also observed that second fraction contributed the maximum in the weight loss.

In another study, Ayllon *et al.* [2005] studied the pyrolysis of MBM in a thermobalance in order to compare different possible kinetic methods to obtain information about the MBM decomposition process. They carried out experiments at different heating rates (5, 10, 15 and 20 °C/ min) with an initial weight of 15 mg, a particle diameter of 250 - 350 µm, a nitrogen flow rate of 100 cm³/ min NTP and a final pyrolysis temperature of 900 °C. They compared different kinetic models, simple kinetic models, which consider the decomposition of one fraction only, models based on several independent fractions decomposing simultaneously with first and second order kinetic equations for each fraction such as two fractions, three fractions and four fractions. They derived the global pyrolysis rate equation as follows:

$$\frac{d\alpha_i}{dT} = \frac{1}{1 - f_\infty} \sum_{i=1}^N \frac{d\alpha_i}{dT} (f_{i0} - f_{i\infty}) \quad (5)$$

Using above equation with right kinetic parameters, the curve for α and the derivative of α with respect to temperature can be simulated. They found the best fitting is obtained with the model that considers four fractions following a second order kinetic law. The respective activation energy was highest for the third fraction and it was 85.9 kJ/ mol.

Miura and Maki [1998] developed a simple method for determining the kinetic parameters for complex reactions such as coal and biomass pyrolysis. This model assumes that a number of parallel, irreversible and first order reactions with different activation energies occur simultaneously. All the reaction activation energies have the same frequency factor, k_0 , at the same conversion rate. According to this model, the release of volatiles is given by:

$$1 - V/V^* = \int_0^\infty \exp(-k_0 \int_0^t e^{-E/RT} dt) f(E) dE \quad (6)$$

Many researchers used distributed activation energy model to study the pyrolysis of coal and biomass and for determining the kinetic parameters as well [Li et al., 2009; Sonobe and Worasuwanarak, 2008]. In this work, the simple distributed activation energy model (DAEM) was used to determine kinetic parameters for pyrolysis of MBM.

Chapter 3

EXPERIMENTAL

This section provides details the experiments conducted in this research. It includes a system description of the experimental approach with schematic diagrams, experimental procedures, analysis of feed, packed bed material, and product gas analysis, and the research plan.

3.1 System description

This section is further divided into two parts for two distinct phases of the research. The first part deals with the system description of phase I: gasification of MBM using oxygen as a gasifying agent in single stage and two-stage reactor systems. The second part deals with the system description of phase II: gasification of MBM using steam as a gasifying agent in single stage and two-stage reactor systems. The third phase: Pyrolysis of meat and bone meal in a thermogravimetric analyzer. The system description is included in the experimental procedure itself.

3.1.1 Phase I: Gasification of Meat and Bone Meal Using Oxygen

Experiments were performed at atmospheric pressure in single stage and two-stage fixed bed reactor systems. A schematic diagram of the apparatus is shown in Fig. 3.1. The first stage and second stage reactors were made of Inconel tubing having 10.5 mm ID and 500 mm and 300 mm lengths respectively. Each reactor had three pins welded inside to support the fixed bed with the help of quartz wool. The reactors were connected by a 3 mm diameter, 40 mm long tube and placed inside separate tubular furnaces. K-type

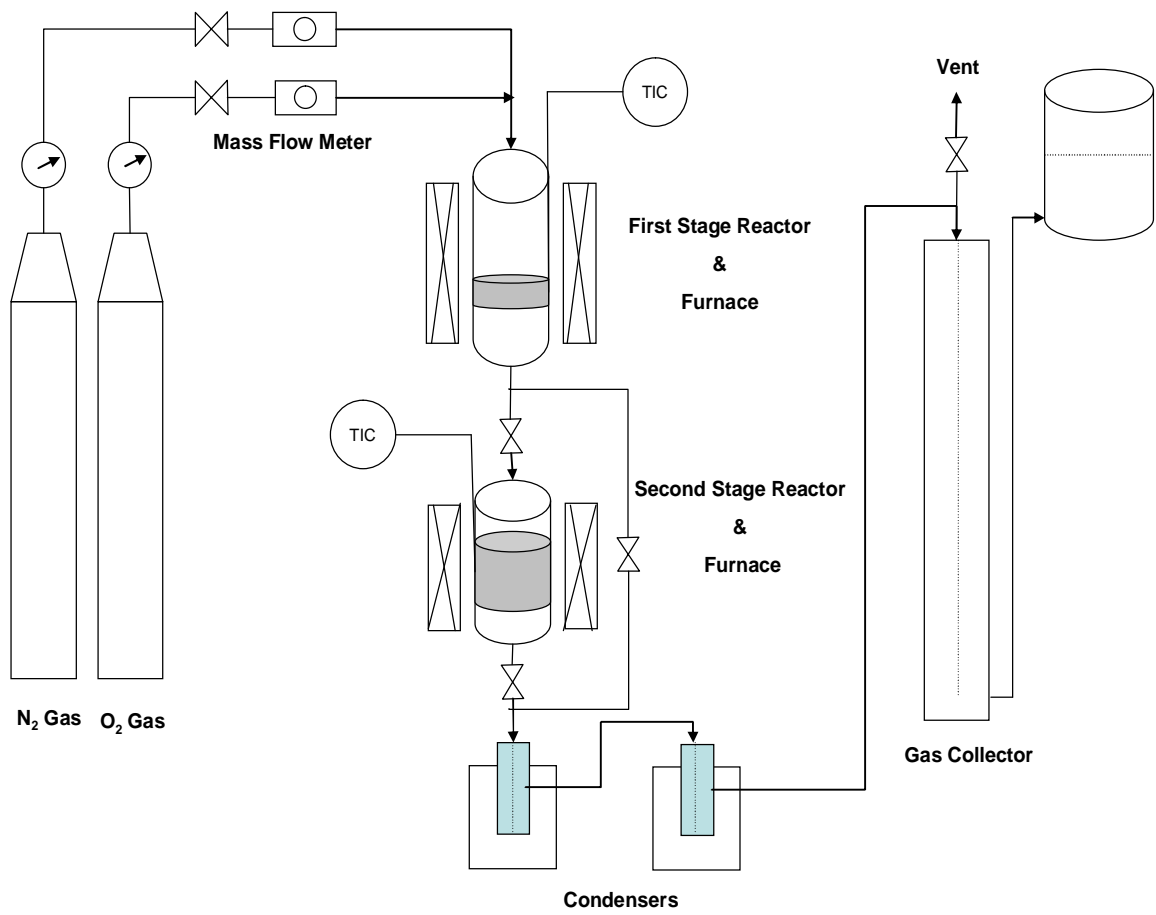


Fig. 3.1 Schematic diagram of experimental setup for gasification of meat and bone meal using oxygen in two-stage fixed bed reaction system

thermocouples were directly connected with each reactor to maintain and monitor the temperature of the reactor wall via temperature controller system (Eurotherm models 2132 and 2416, USA). Nitrogen as an inert carrier gas and oxygen as a gasifying agent were supplied at the desired flow rates from separate cylinders through needle valves and mass flow meters (Aalborg model GFM17). The calibration of the mass flow meters was carried out using a calibrated bubble flow meter and is presented in Appendix A. Two glass condensers in series below the second stage reactor, surrounded by a mixture of ice and salt, were used to condense the tar and cool down the product gases. The product gases were collected in the saturated brine solution column which was further connected to the overhead surge tank to receive the displaced brine solution.

3.1.2 Phase II: Gasification of Meat and Bone Meal Using Steam

Experiments were performed at atmospheric pressure in single stage and two-stage fixed bed reactor systems. The schematic diagram is shown in Fig. 3.2. The first stage and second stage reactors were made up of Inconel tubing having 10.5 mm ID and 500 mm and 370 mm lengths respectively. Each reactor had three pins welded inside to support the fixed bed with the help of quartz wool. The reactors were connected by a 3 mm diameter, 40 mm long tube and placed inside separate split tube furnaces (Applied Test Systems, Inc., USA) with thermocouples located at the mid-length of the heating zone. The temperatures of the reactors were monitored and controlled by temperature controller system (Eurotherm models 2132 and 2416, USA). Nitrogen as an inert carrier was supplied at the desired flow rate from a separate cylinder through a needle valve and mass flow meter (Aalborg model GFM17), while water was injected into the reactor by a syringe pump (Kent Scientific, Genie Plus

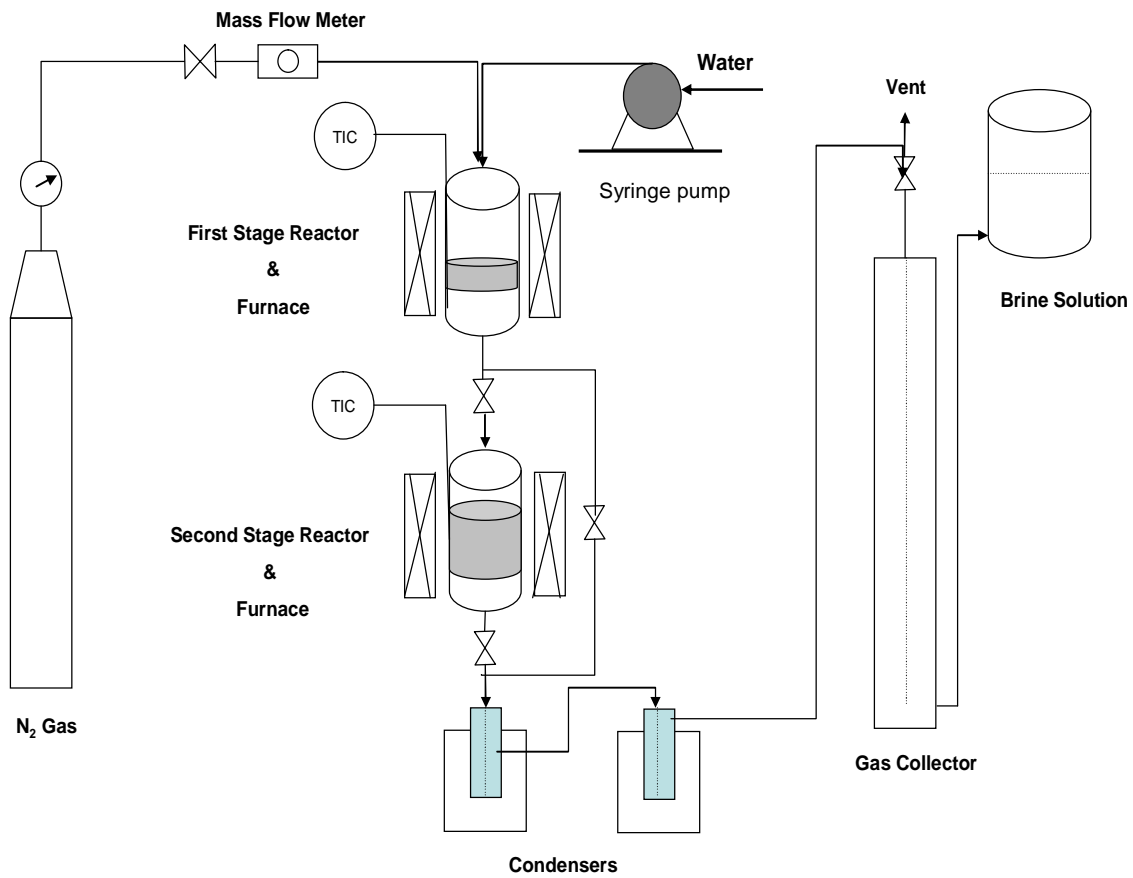


Fig. 3.2 Schematic diagram of experimental setup for steam gasification of meat and bone meal in two-stage fixed bed reaction system

Model, USA) at the desired flow rate. The calibration curve is presented in Appendix A. Two glass condensers in series below the second stage reactor, surrounded by a mixture of ice and salt, were used to condense the tar and cool down the product gases. The product gases were collected in the saturated brine solution column to prevent CO₂ dissolution in pure water. The brine solution column was further connected to the overhead surge tank to receive the displaced brine solution.

3.2 Experimental procedure

3.2.1 Phase I: Gasification of Meat and Bone Meal Using Oxygen

The first stage was used for gasification of MBM while the second stage was used for further cracking of tar. The feed material was placed inside the first stage reactor and inert packed bed material (Ottawa sand) was placed inside the second stage reactor. These materials were supported on the plug of quartz wool which was held on the supporting pins inside each reactor. The sample size of MBM was 2 g for all experiments. The heating rate of the first stage reactor was kept at 25 °C /min. The oxygen supply was started when the first stage reactor temperature reached to 50 °C. It then took 24 to 32 min from 50 °C to reach the final temperature of 650 to 850 °C in the case of single stage experiments. In the case of two-stage experiments, the second stage reactor was heated to the desired temperature (650-850 °C) before the heating of first stage started. The heating of first stage was started at 25 °C /min. The remainder of the experimental procedure was the same as single stage experiments. After attaining the final desired temperature of the first stage, the reaction was allowed to continue for the next 30 min. Subsequently the heating was stopped and the reactor(s) was allowed to cool down. The amount of product gases collected was measured by the

displacement of the brine solution. They were analyzed using two different gas chromatographs (GCs HP 5880 and HP 5890). The amount of condensed tar in the glass condensers and the char left inside the reactor were measured by taking the difference in weights of glass condensers and reactor before and after the reaction. After each run, the reactor and glass condensers were cleaned using acetone and then dried with compressed air prior to the next run.

3.2.2 Phase II: Gasification of Meat and Bone Meal Using Steam

The first stage was used for gasification of MBM while the second stage was used for further cracking of tar. The feed material was placed inside the first stage reactor and inert packed bed material (Ottawa sand) was placed inside the second stage reactor. These materials were supported on the plug of quartz wool which was held on the supporting pins inside each reactor. The sample size of MBM was kept 2 g for all experiments. The heating rate of the first stage reactor was kept at 25 °C /min. Water injection was started when the first stage reactor temperature reached 110 °C. It took approximately 25 to 33 min from 30 °C to reach the final temperature of 650 to 850 °C in the case of single stage experiments. In the case of two-stage experiments, the second stage reactor was heated to the desired temperature (650-850 °C) with N₂ flow of 45 ml/min before the heating of first stage started. The heating of first stage was started at 25 °C /min. The remainder of the experimental procedure was the same as in case of single stage experiments. After attaining the final desired temperature of the first stage, the reaction was allowed to continue for the next 30 min. Subsequently the heating was stopped and the reactor(s) allowed to cool down. The amount of product gases collected was measured by the displacement of the brine solution.

They were analyzed using two different gas chromatographs (GCs HP 5880 and HP 5890). The amount of condensed liquid (tar + water) in the glass condensers and the char left inside the reactor were measured by a weight difference before and after the reaction. After each run, the reactor and glass condensers were cleaned using acetone and then dried with compressed air prior to the next run.

3.2.3 Phase III: Pyrolysis of Meat and Bone Meal in a Thermogravimetric Analyzer

The thermogravimetric analyzer (Pyris Diamond TG/ DTA, PerkinElmer Instruments, USA) consists of a micro thermobalance with an electric furnace connected to a computer. Argon was used as a carrier gas to sweep the product gases. Its flow rate was set at 60 ml/min as per the operating procedure of the instrument. The MBM sample was kept in a Alumina sample holder. The sample size was kept 10 mg approximately in all experiments. The final pyrolysis temperature of the sample in all experiments was set at 550 °C. The experiments were carried out at three different heating rates (10, 15, and 25 °C/ min).

3.3 Analysis of meat and bone meal, inert packed bed material, and product gases

Experiments were performed with meat and bone meal obtained in the powder form from Saskatoon Processing Ltd., Saskatoon, SK, Canada. The particle size distributions of the meat and bone meal and the inert packed bed material (Ottawa sand), in the second stage reactor were carried out using a particle size analyzer (MasterSizer, Malvern Instruments, UK). The MBM was filled without applying any pressure or tapping in a standard volume cylindrical container. Then, the cylindrical container was weighed and the difference in weights of filled and empty container was used to calculate the specific gravity of MBM. The

proximate analysis of MBM was carried out using ASTM D 3172-89 standards while the elemental analysis was carried out using a Vario EL III CHNS analyzer (Elementar Americas Inc., USA). The product gases were analyzed using two different gas chromatographs (GCs HP 5880 and HP 5890). The HP 5880 was equipped with a flame ionization detector (FID). A Chromosorb 102 column with 1/8 inch diameter and 6 ft length was used to analyze the CH₄ and other hydrocarbons. The HP 5890 was equipped with a thermal conductivity detector (TCD). A Carbosieve S II column with 1/8 inch diameter and 10 ft length was used to analyze H₂, CO and CO₂. The conditions for the HP 5880 were as follows: initial temperatures of 40 °C, initial temperature hold time of 1 min, heating rate of 10 °C /min., final temperature of 180 °C, final hold time of 3 min., injector temperature of 220 °C and detector temperature of 250 °C. The conditions for the HP 5890 were as follows: initial temperatures of 40 °C, initial temperature hold time of 1 min, heating rate of 10 °C /min, final temperature of 180 °C, final hold time of 3 min, injector temperature of 200 °C and detector temperature of 220 °C. The gas analysis was carried out on a carrier gas (N₂) free basis.

3.4 Experimental design

Semi-batch gasification of MBM in phases I and II was carried out by studying the effect of one parameter at a time while holding all other parameters constant. The range of the parameters was selected based on the literature review and experimental set up limitations and is shown in Table 3.1. The optimum run, which was selected based on the highest hydrogen/ syngas yield, was repeated once for each parameter to find out the percentage difference in reproducibility of the experimental data.

Table 3.1 Experimental design

	Parameter	Range	T₁	T₂	ER	Steam/ MBM	Packed bed height
Phase I	T ₁	650-850 °C	650-850 °C	-	0.2	NA	60
	T ₂	650-850 °C	650-850 °C	650-850 °C	0.2	NA	60
	ER	0.15-0.3	650-850 °C	650-850 °C	0.15-0.3	NA	60
	Packed bed height	40-100 mm	650-850 °C	650-850 °C	0.15-0.3	NA	40-100 mm
Phase II	T ₁	650-850 °C	650-850 °C	-	NA	0.6	60
	T ₂	650-850 °C	650-850 °C	650-850 °C	NA	0.6	60
	Steam/ MBM	0.2-0.8	650-850 °C	650-850 °C	NA	0.2-0.8	60
	Packed bed height	40-100 mm	650-850 °C	650-850 °C	NA	0.2-0.8	40-100 mm

T₁: Temperature of 1st stage; T₂: Temperature of 2nd stage; ER: Equivalence ratio; NA: Not applicable

Chapter 4

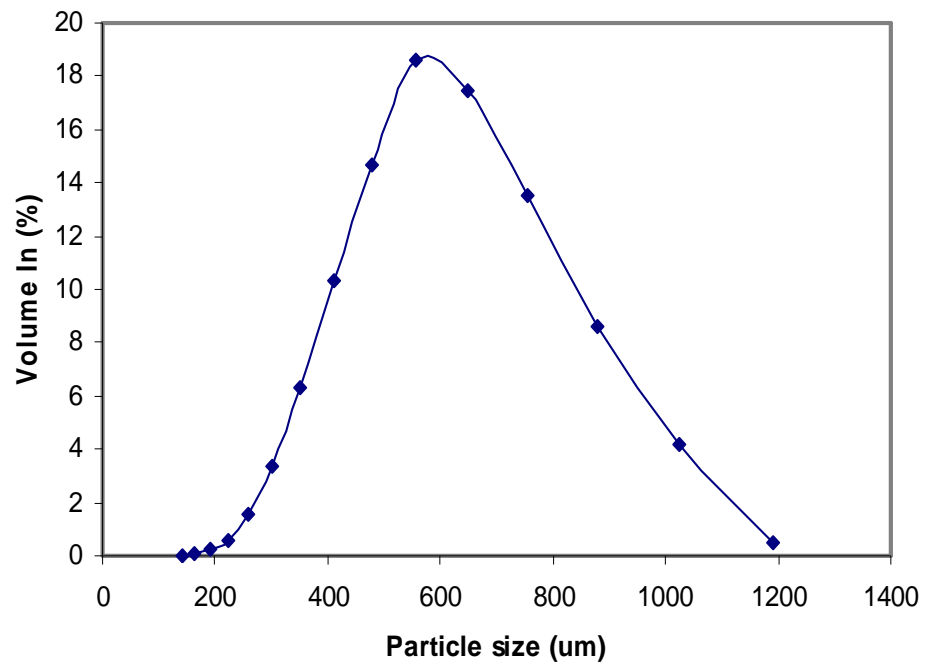
RESULTS AND DISCUSSION

This chapter presents the experimental results and discussion from phases I to III of the project. Section 4.1 deals with the proximate and elemental analysis of the MBM as well as particle size distribution of MBM and Ottawa sand used in the experiments. The results and discussion of the effects of different parameters during the gasification of MBM using oxygen are presented in section 4.2. Section 4.3 presents results from the steam gasification of MBM, while section 4.4 consists of determination of kinetic parameters for the pyrolysis of MBM in a thermogravimetric analyzer.

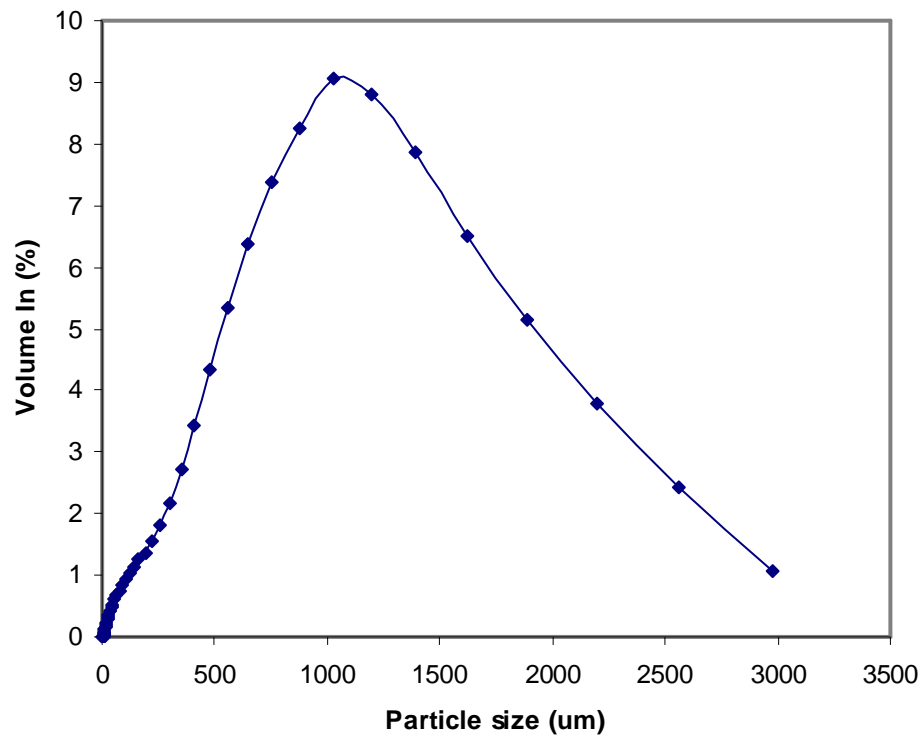
Optimal experiments were repeated for each parameter to check the reproducibility of the data. Percentage difference observed in replicate runs is reported in each figure. The variation observed in product yield and gas composition during replicate runs is considered to be mainly due to non-homogeneity of meat and bone meal in the sample and errors during product yield and gas analyses.

4.1 Particle size distribution, proximate and elemental analysis

The MBM used for the experiments was in powder form and brownish in color having specific gravity of approximately 0.55. The particle size distribution of Ottawa Sand and MBM powder was carried out using MasterSizer and it is in the range of 152.2 to 1290.9 μm and 5 to 3228 μm respectively as shown in Fig. 4.1 (a) and (b). The proximate analysis of MBM is presented in Table 4.1. The carbon (C), hydrogen (H), nitrogen (N) and sulfur (S) analysis of the MBM is also presented in Table 4.1. The gross heating value of MBM was



(a)



(b)

Fig. 4.1 Particle size distributions of (a) Ottawa sand and (b) MBM powder

Table 4.1 Proximate and ultimate analysis of meat and bone meal

Moisture content (wt. % wet basis)	4.5
Gross heating value (MJ/kg)	17.1
Proximate analysis (wt. % dry basis)	
Volatile matter	73.8
Ash	18.3
Fixed Carbon	7.8
Ultimate analysis (wt. %)	
C	46.3
H	6.6
N	9.7
S	1.0
O ^a	36.4

^a = by difference

calculated using the Channiwala and Parikh [2002] correlation. The results are comparable with the literature. The carbon, hydrogen, and nitrogen contents of MBM in the literature were in the range of 41 to 46 (wt. %), 5.8 to 6.4 (wt. %), and 7.8 to 9 (wt. %). Moreover, the gross heating value mentioned in the literature was in the range of 17-20 MJ/kg which is also comparable with the heating value of MBM used in this work [Chaala and Roy, 2003; Ayllon *et al.*, 2006; Conesa J.A. *et al.*, 2003].

4.2 Gasification of meat and bone meal using oxygen

4.2.1 Single stage operation

4.2.1.1 Effect of temperature

The effect of final temperature of the first stage was studied by bypassing the second stage in Fig. 3.1. The final temperature of first stage was varied from 650 to 850 °C in increments of 50 °C while holding equivalence ratio (ER) at 0.2 and nitrogen flow rate at 45 ml/min. The effect of the final temperature of the first stage on product (char, tar and gas) yield and gross heating value (GHV) of gas is presented in Fig. 4.2. As expected, char (from 22.9 to 17.8 wt. %) and tar (from 47 to 40.7 wt. %) yields decreased, while gas yield increased (from 22.1 to 30.8 wt. %). Higher temperature is favorable for the gasification of char as well as thermal cracking of tar. Similar trends were observed by Lv *et al.* [2004]. They found that carbon conversion increased from 1.43 to 2.53 Nm³/kg biomass when the reactor temperature increased from 700 to 900 °C in air-steam gasification of pine sawdust in a fluidized bed.

Fig. 4.3 shows the effect of the final temperature of the first stage on gas composition. The product gas was mainly composed of H₂, CO, CO₂, CH₄ and other heavier hydrocarbon

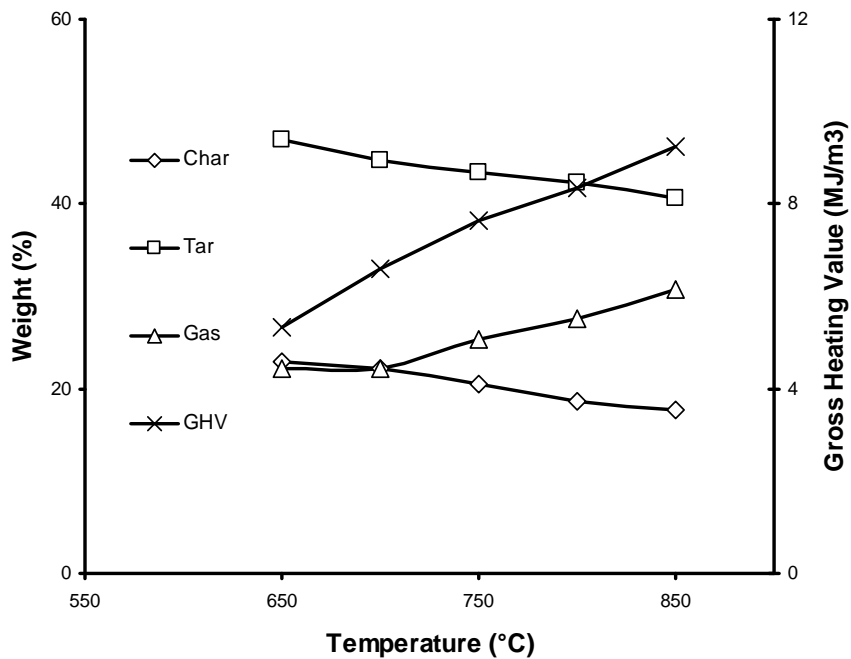


Fig. 4.2 Effect of first stage final temperature on product yield and GHV of gas at ER of 0.2 and N₂ flow rate of 45 ml/min (% Difference in replicate run: Char - ±2, Tar - ±2, Gas - ±4)

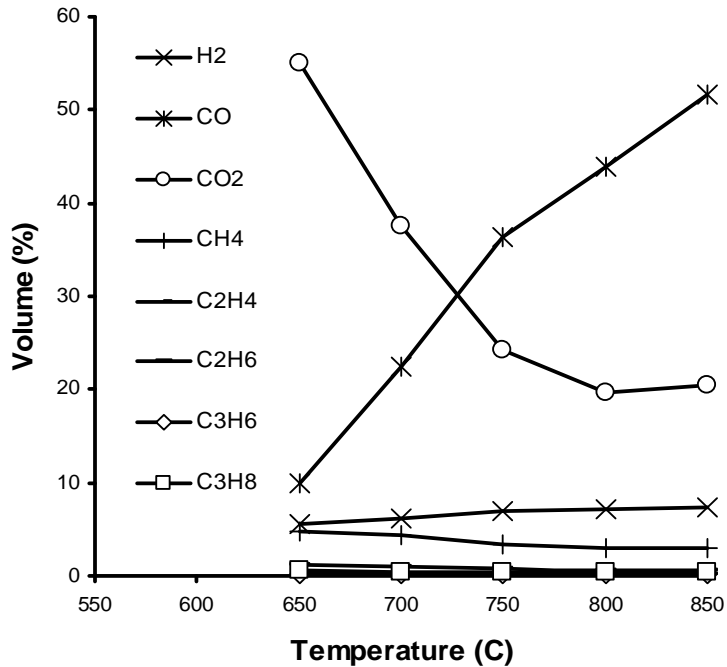


Fig. 4.3 Effect of final temperature of first stage on gas composition at ER of 0.2 and N₂ flow rate of 45 ml/min (% Difference in replicate run: H₂ - ±3, CO - ±4, CO₂ - ±6, CH₄ - ±2, Other H/C - ±3)

gases. Each gas component showed a clear trend. The H₂ yield increased from 5.5 to 7.3 vol. % (N₂ free basis), the CO₂ yield decreased sharply from 55 to 20.5 vol. % and CO yield increased remarkably from 10 to 51.6 vol. % with an increase in temperature from 650 to 850 °C. Enhanced carbon conversion and the Boudard reaction ($C + CO_2 \rightarrow 2CO$), reaction of carbon and carbon dioxide to produce carbon monoxide, at higher temperature are partially responsible for the observed increase in CO and the corresponding decrease in CO₂. The gasification of biomass is a very complex process. It involves several physical and chemical steps [Cipriani *et al.*, 1998]. Methane and other hydrocarbons showed little variation with an increase in temperature. This is likely due to some secondary reactions with CO₂. The gross heating value (GHV) of the product gases increased from 5.3 to 9.3 MJ/m³ as temperature increased from 650 to 850 °C, which is consistent with the significant increase in CO content in the product gas.

4.2.2 Two - stage operation

4.2.2.1 Effect of temperature

Tar is a complex mixture of condensable hydrocarbons, which includes single ring to multiple ring aromatic compounds along with other oxygen containing hydrocarbons and complex polycyclic aromatic compounds [Devi *et al.*, 2005]. The tar can be removed in various ways, with increased residence time and thermal cracking being two of them [Bridgwater, 1995]. With this in mind, second stage reactor was introduced in series to the first stage for further cracking of tar and to increase the H₂ yield. The second stage reactor temperature was varied from 650 to 850 °C in increments of 50 °C, keeping first stage temperature at 850 °C, equivalence ratio (ER) at 0.2, nitrogen flow rate at 45 ml/min.

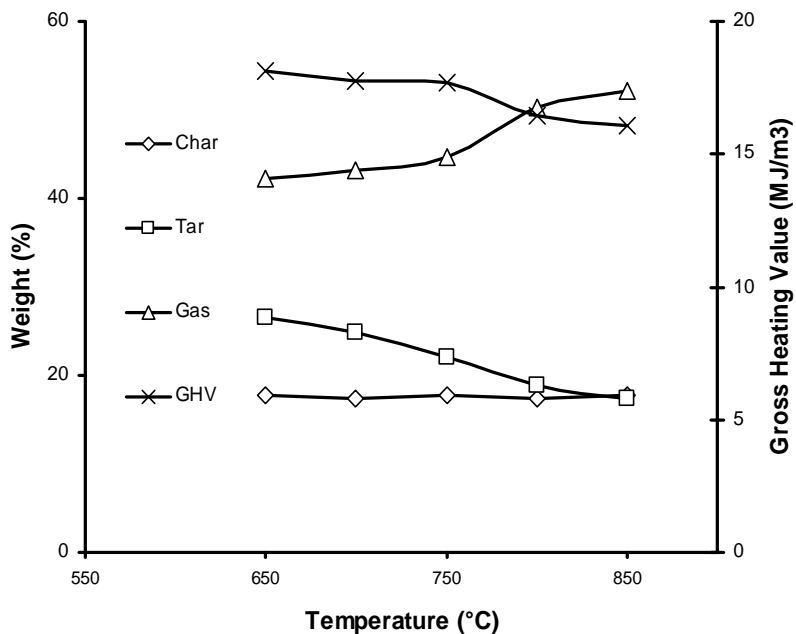


Fig. 4.4 Effect of second stage temperature on product yield and GHV of gas at first stage final temperature of 850 °C, ER of 0.2, N₂ flow rate of 45 ml/min and packed bed height of 60 mm (% Difference in replicate run: Char - ±2, Tar - ±2, Gas - ±4)

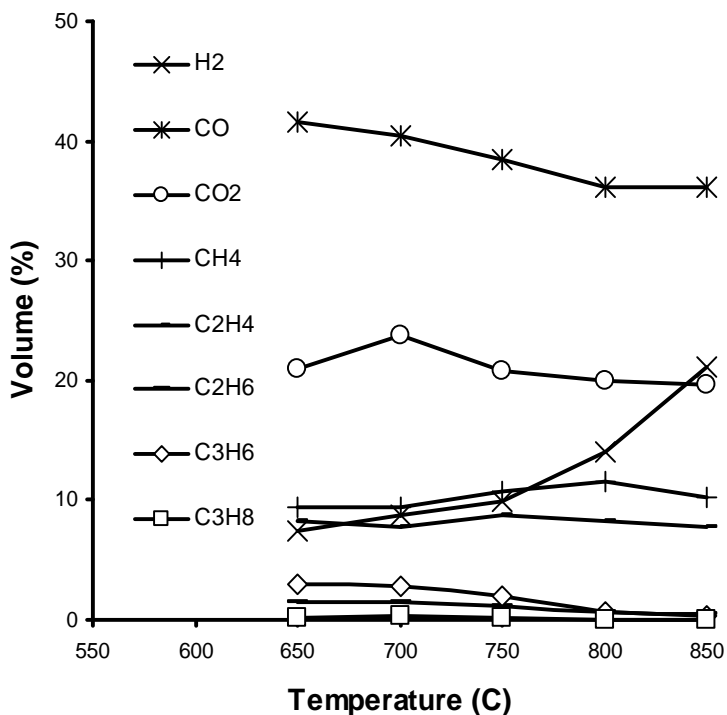


Fig. 4.5 Effect of second stage temperature on gas composition at first stage final temperature of 850 °C, ER of 0.2, N₂ flow rate of 45 ml/min and packed bed height of 60 mm (% Difference in replicate run: H₂ - ±3, CO - ±1, CO₂ - ±7, CH₄ - ±5, Other H/C - ±4)

The second stage also contained a packed bed of inert material (Ottawa sand) packed to depth of 60 mm.

The effect of second stage temperature on product yield is presented in Fig. 4.4. The tar yield decreased from 26.5 to 17.4 wt. % and gas yield increased from 42.3 to 52.2 wt. %. The decrease in tar yield and increase in gas yield were 16.4 and 5.6 % respectively up to 750 °C but beyond this temperature, they were 21.4 and 16.8 %, respectively. This shows that the thermal cracking of tar becomes highly favorable beyond 750 °C. By introducing the second stage, the tar yield is reduced by 57.3 % while gas yield is 40.9 % higher than that obtained using only a single stage. Fig. 4.5 shows that CO content decreased consistently from 41.6 to 36.2 vol. %, while that of CO₂ showed no consistent change. The CH₄ yield increased slightly at temperatures above 700 °C, while the yield of C₂₊ hydrocarbons (C₂H₆, C₃H₆, C₃H₈) decreased sharply after 700 °C. This phenomenon can be explained as cracking of heavier hydrocarbons into lighter hydrocarbons and H₂ which is further supported by the rapid increase in H₂ content after 700-750 °C. The gross heating value (GHV) of product gases decreased gradually from 18.1 to 16.1 MJ/m³ over the temperature range of 650 to 850 °C because of the continuous decrease in heavier hydrocarbon yield.

4.2.2.2 Effect of equivalence ratio

The equivalence ratio is defined as the air to fuel weight ratio used in the gasification process divided by the air to fuel weight ratio for stoichiometric combustion [Narvaez *et al.*, 1996]. From the ultimate analysis of Table 4.1, elemental formula of MBM (CH_{1.7}O_{0.59}N_{0.18}) was derived to set up the oxidation reaction, which was used to calculate the equivalence ratio: CH_{1.7}O_{0.59}N_{0.18} + mO₂ → CO₂ + nH₂O + pNO₂ [Zhu and Venderbosch, 2005]. In

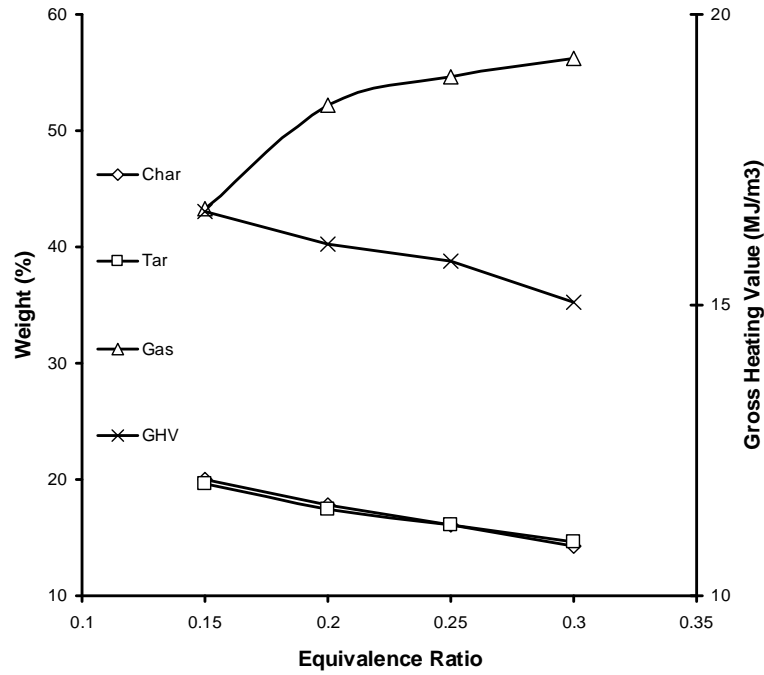


Fig. 4.6 Effect of equivalence ratio (ER) on product yield and GHV of gas at first stage final and second stage temperatures of 850 °C and packed bed height of 60 mm (% Difference in replicate run: Char - ± 2 , Tar - ± 2 , Gas - ± 2)

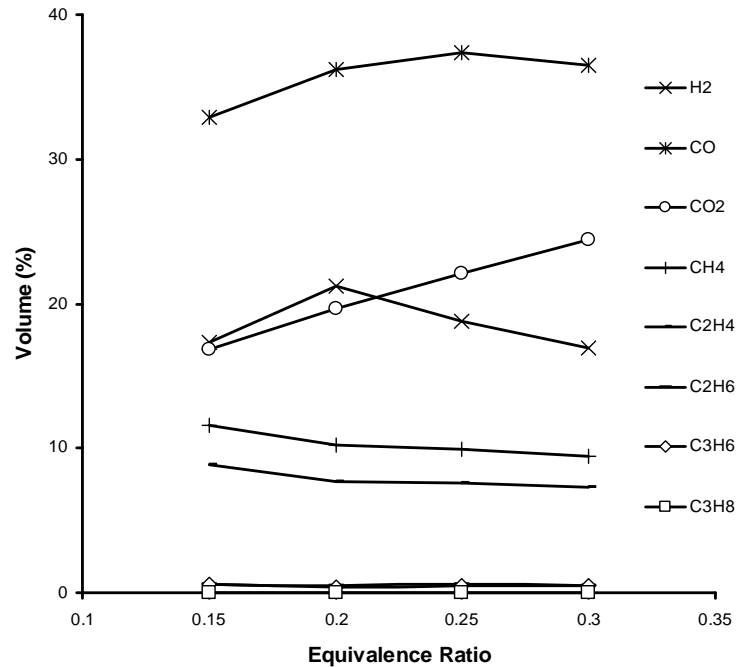


Fig. 4.7 Effect of equivalence ratio (ER) on gas composition at first stage final and second stage temperatures of 850 °C and packed bed height of 60 mm (% Difference in replicate run: H₂ - ± 3 , CO - ± 1 , CO₂ - ± 7 , CH₄ - ± 5 , Other H/C - ± 4).

the present work, ER was varied from 0.15 to 0.3 in increments of 0.05, keeping the final temperature of the first and second stages at 850 °C and the packed bed height in the second stage at 60 mm. The nitrogen flow rate was varied accordingly to compensate for the variation in oxygen flow rate and hence keep the total volumetric flow rate of gas entering to the system constant. The effect of ER on product distribution and gas composition is presented in Fig. 4.6 and 4.7. It was observed that with increase in ER, char and tar yield decreased from 20 to 14.2 wt.% and 19.6 to 14.6 wt.% respectively while gas yield increased from 43.3 to 56.2 wt.%. The gross heating value (GHV) of the gases decreased slightly from 16.6 to 15 MJ/m³. The increase in ER promotes oxidation reactions and deteriorates the product gas quality. It was observed that H₂ content in the product gas reached a maximum value of 21.2 vol. % at an ER of 0.2 and then dropped to 16.9 vol. % with further increase in ER. Increase in CO₂ content from 16.8 vol. % to 24.4 vol. % can be explained by strong oxidation reaction. The CH₄ and C₂H₄ content in the product gas were decreased marginally from 11.6 to 9.4 and 8.9 to 7.3 vol. % respectively. There was no significant changes observed in case of higher hydrocarbon gases. Similar trends were reported by other researchers [Manya *et al.*, 2006; Mansaray *et al.*, 1999]. Manya *et al.* [2006] observed that with increase in air ratio (ER) from 24 to 35 %, the concentrations of H₂, CO, CH₄, C₂H₄, and C₂H₆ decreased in air gasification of sewage sludge in a bubbling fluidized bed. Mansaray *et al.* [1999] observed that as equivalence ratio was increased, the concentration of CO₂ increased while the concentration of the flue gases (H₂, CO, CH₄, C₂H₂ + C₂H₄, and C₂H₆) decreased.

4.2.2.3 Effect of packed bed height

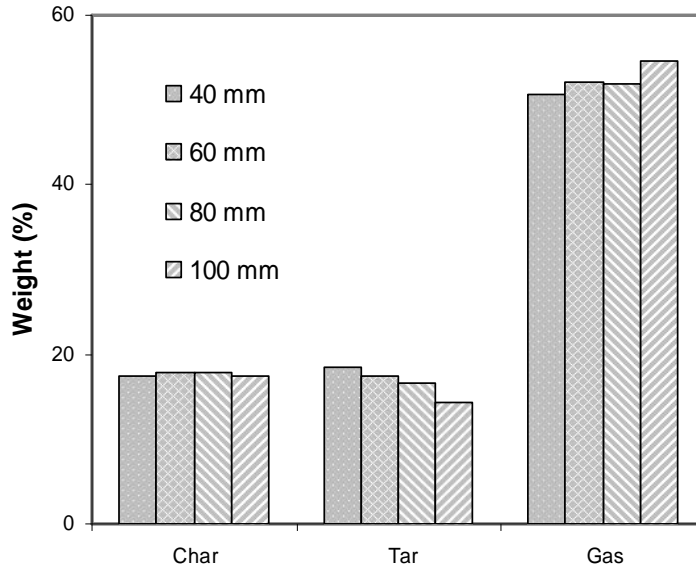


Fig. 4.8 Effect of packed bed height on product yield at first stage final and second stage temperatures of 850 °C, ER of 0.2 and N₂ flow rate of 45 ml/min (% Difference in replicate run: Char - ±2, Tar - ±3, Gas - ±2)

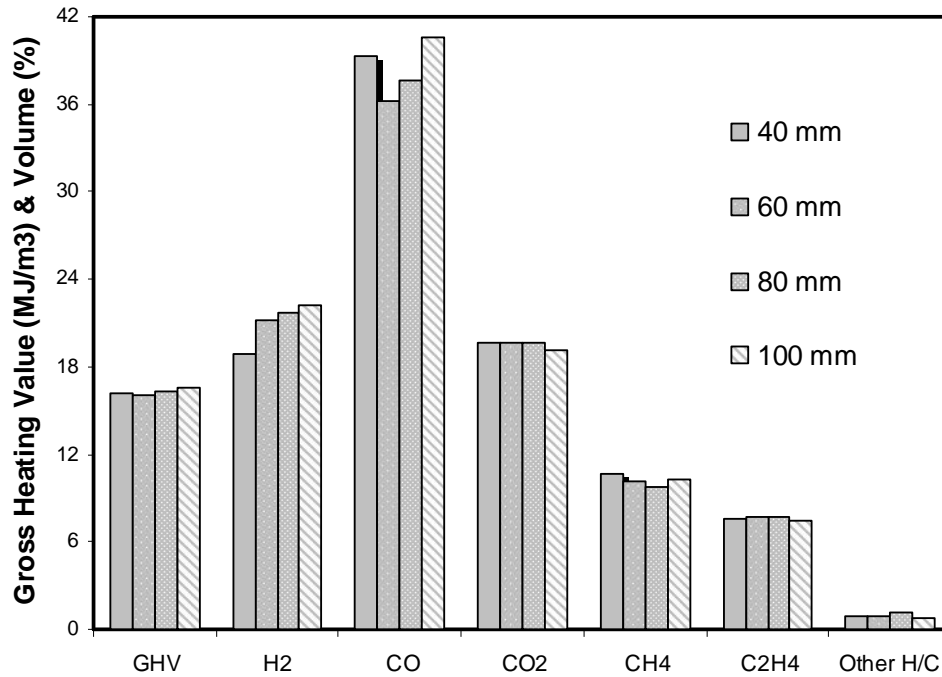


Fig. 4.9 Effect of packed bed height on gas compositions and gross heating value at first stage final and second stage temperatures of 850 °C, ER of 0.2 and N₂ flow rate of 45 ml/min (% Difference in replicate run: H₂ - ±1, CO - ±3, CO₂ - ±1, CH₄ - ±3, Other H/C - ±1)

The residence time of the tar can be changed by changing the packed bed height of cracking stage. Higher residence time is favorable for the thermal cracking of tar, and higher hydrocarbons, as well as for allowing secondary reactions to take place. In the present work, the packed bed height in the second reactor was varied from 40 to 100 mm keeping the final temperature of the first and second stages at 850 °C, ER at 0.2, and N₂ flow rate at 45 ml/min. Fig. 4.8 and 4.9 show the product yield and gas compositions as a function of packed bed height. It can be deduced that an increase in packed bed height decreased tar yield from 18.6 to 14.2 wt.% and increased gas yield from 50.6 to 54.6 wt.%. The H₂ content increased slightly from 18.9 to 22.3 vol. %, while CO content initially decreased from 39.3 to 36.2 vol. % and then increased up to 40.7 vol. %. There was a little variation observed in the case of CO₂ content. It was almost constant in the range of 19.7 to 19.2 vol. % with increase in packed bed height from 40 to 100 mm. CH₄ yield decreased slightly from 10.7 to 9.8 vol. % with packed bed height from 40 to 80 mm and then increased little up to 10.3 vol. % at packed bed height of 100 mm. The yield of C₂H₄ was almost constant in the range of 7.6 to 7.5 vol. % over the packed bed height from 40 to 100 mm. Other heavier hydrocarbons (C₂H₆, C₃H₆ and C₃H₈) combined showed opposite trend than CH₄. They first increased slightly from 0.8 to 1.2 vol. % and then decreased to 0.8 vol. % with increase in packed bed height. An initial increase in heavier hydrocarbons could be because of cracking of tar into heavier hydrocarbon gases and then decrease of them could be explained by further cracking into CH₄ and H₂. Xiao *et al.* [2007] studied the effect of bed height in air gasification of polypropylene plastic waste in fluidized bed gasifier. They found that tar and heavier hydrocarbons yield decreased while gas yield increased with increase in bed height.

4.3 Gasification of meat and bone meal using steam

4.3.1 Single stage operation

4.3.1.1 Effect of temperature

The effect of final temperature of the first stage was studied by bypassing the second stage reactor of Fig. 3.2. In the present work, the final temperature of first stage was varied from 650 to 850 °C with increments of 50 °C, while maintaining a steam/ MBM (wt. /wt.) ratio of 0.6 and a N₂ flow rate of 45 ml/min. The effect of final temperature of the first stage on product (char, liquid and gas) yield gas composition is presented in Figs. 4.10 and 4.11. As expected, char (from 21.7 to 14.1 wt. %) and liquid (tar + water) (from 57.9 to 52.2 wt. %) yields decreased, whereas gas yield increased (from 8.7 to 18.1 wt. %) with an increase in temperature from 650 to 850 °C. It was also observed that after 750 °C, gas production was rapid which shows that gasification reactions become significant after 750 °C. This could be explained by higher char conversion with steam and thermal cracking/steam reforming of tar at the higher temperature. Similar trends were obtained by other researchers [Ferdous *et al.*, 2001; Franco *et al.*, 2003]. Ferdous *et al.* [2001] found that when the temperature of fixed bed reactor was increased from 650 to 800 °C, lignin conversion increased from 56 to 69 wt. % and from 60 to 76 wt. % for Alcell and Kraft lignin, respectively. Franco *et al.* [2003] observed an increase in gas yield and decrease in tar and char yield while increasing in temperature from 700 to 900 °C during steam gasification of forestry biomass in an atmospheric fluidized bed. The product gas was mainly composed of H₂, CO, CO₂, CH₄ and other heavier hydrocarbon gases. The H₂ and CO yields increased from 42 to 52.2 vol. % and 10.2 to 26.8 vol. % (N₂ free basis) respectively while that of CO₂ decreased sharply from 25.9 to 12.8 vol. % with increase in temperature from 650 to 850 °C. Increased carbon

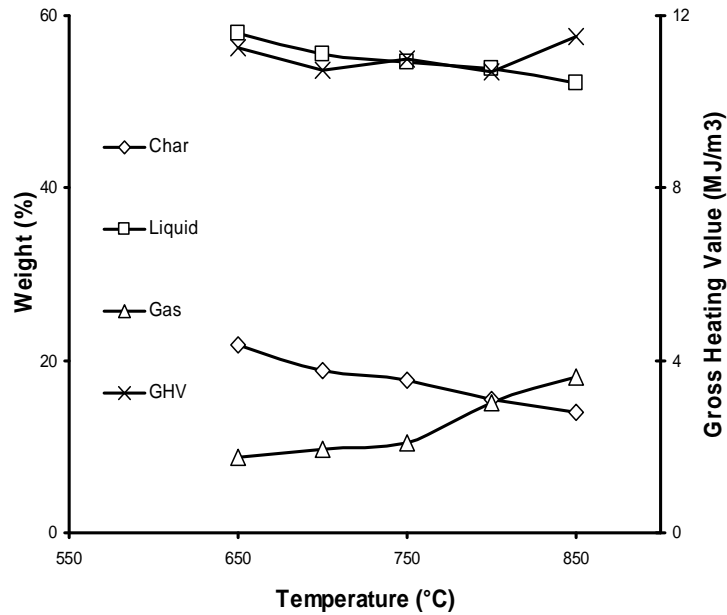


Fig. 4.10 Effect of final temperature of first stage on product yield (wt. % yield) at steam/MBM (wt. /wt.) of 0.6 and N₂ flow rate of 45 ml/min (% Difference in replicate run: Char - ±2, Liquid - ±2, Gas - ±4)

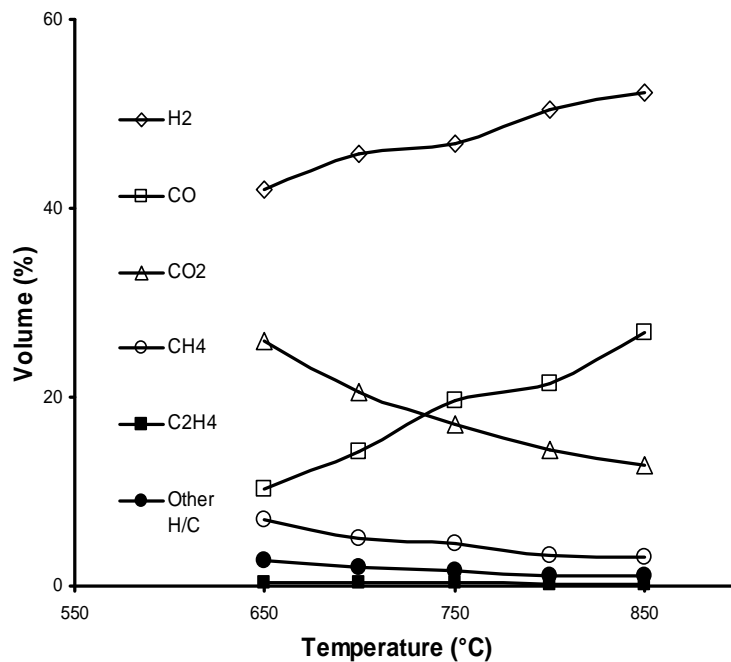


Fig. 4.11 Effect of final temperature of first stage on gas composition (volume % yield (N₂ free basis)) at steam/MBM (wt. /wt.) of 0.6 and N₂ flow rate of 45 ml/min (% Difference in replicate run: H₂ - ±1, CO - ±6, CO₂ - ±2, CH₄ - ±1, Other H/C - ±3)

conversion as well as Boudard reaction, ($C + CO_2 \rightarrow 2CO$) are partially responsible for the observed increase in CO and decrease in CO₂ content at higher temperature. CH₄ (from 7 to 3.1 vol. %) and other hydrocarbons (from 2.7 to 1 vol. %) showed a marginal decrease with an increase in temperature. This could be explained by the likelihood of some secondary reactions with CO₂ as well as steam reforming reaction of hydrocarbons to produce CO and H₂. The gross heating value of product gases was almost constant in the range of 11.2 - 11.5 MJ/m³.

4.3.2 Two - stage operation

4.3.2.1 Effect of temperature

The tar product observed above can be removed by increasing in the gas residence time thus facilitating thermal cracking [Bridgwater, 1995]. Hence, the second reactor stage was introduced in series to the first stage for further cracking/ reforming of tar and to increase the H₂ yield.

The second stage reactor temperature was varied from 650 to 850 °C with increments of 50 °C keeping temperature of first stage at 850 °C, steam/ MBM (wt. /wt.) at 0.6, nitrogen flow rate at 45 ml/min and packed bed height at 60 mm. The effect of temperature of second stage on product yield and gas composition is presented in Figs. 4.12 and 4.13. The liquid (tar + water) yield decreased from 39.1 to 32.4 wt. % and gas yield increased from 26.8 to 32.1 wt. % as second stage temperature increased from 650 to 850 °C. After introducing the second stage, the liquid (tar + water) yield is 37.9 % lower while gas yield is 77.3 % greater than that obtained using only a single stage reactor system. H₂ yield increased from 39.9 to 46.2 vol. % while that of CO and CO₂ were almost constant over the range of 23.6 - 23.9 and

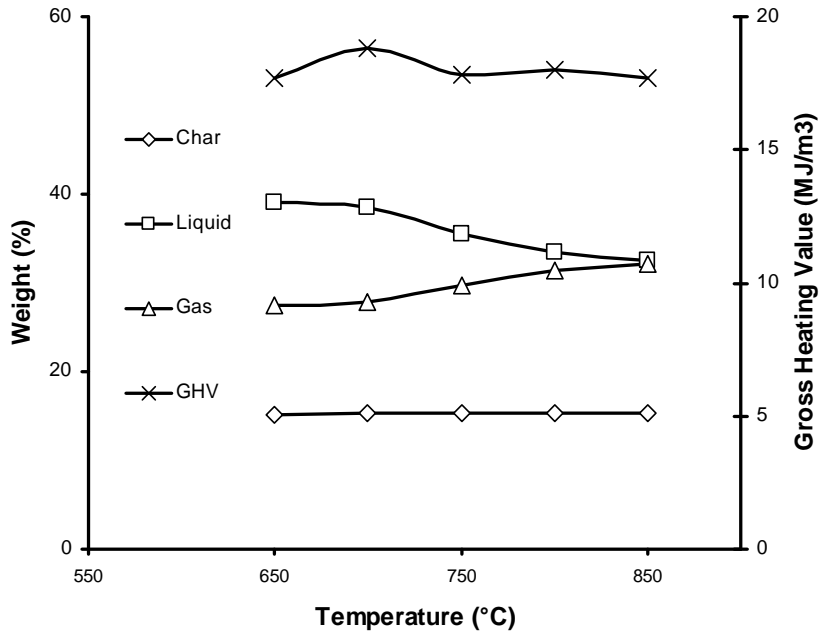


Fig. 4.12 Effect of second stage temperature on product yield (wt. % yield) at first stage final temperature of 850 °C, steam/MBM (wt. /wt.) of 0.6, N₂ flow rate of 45 ml/min and packed bed height of 60 mm (% Difference in replicate run: Char - ±2, Liquid - ±2, Gas - ±1)

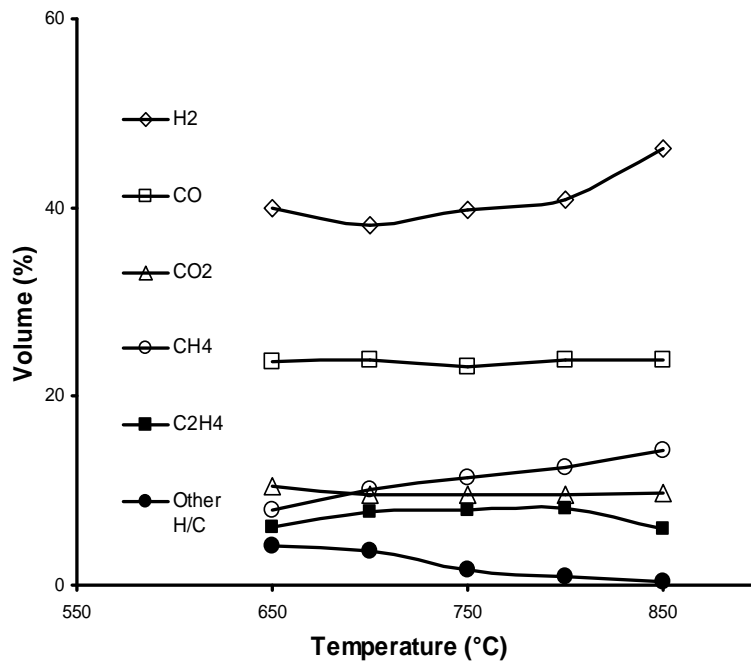


Fig. 4.13 Effect of second stage temperature on gas composition (volume % yield (N₂ free basis)) at first stage final temperature of 850 °C, steam/MBM (wt. /wt.) of 0.6, N₂ flow rate of 45 ml/min and packed bed height of 60 mm (% Difference in replicate run: H₂ - ±2, CO - ±5, CO₂ - ±4, CH₄ - ±6, Other H/C - ±6)

10.5 - 9.8 vol. % respectively. The CH₄ yield increased linearly from 7.8 to 14.2 vol. % with increasing in temperature, while C₂H₄ increased from 5.1 to 8.2 vol. % up to 800 °C and then decreased to 5.9 vol. %. Other heavier hydrocarbons decreased sharply after 700 °C. This phenomenon can be explained by the reforming/cracking of heavier hydrocarbons into light gases. The gross heating value initially increased up to 18.8 MJ/m³ and then dropped down to 17.5 MJ/m³ with increase in temperature which is consistent with the sharp decrease in heavier hydrocarbons content.

4.3.2.2 Effect of steam to meat and bone meal ratio

In this set of experiments, the steam/ MBM ratio (wt/ wt) was varied from 0.2 to 0.8 while keeping the final temperature of the first and second stages at 850 °C, N₂ flow rate at 45 ml/min, and packed bed height of the second stage at 60 mm. The effect of steam/ MBM on product yield and gas composition is presented in Figs. 4.14 and 4.15. The char yield decreased from 27 to 13 wt. % while liquid (tar + water) and gas yields increased from 29.2 to 36.7 and 23.6 to 30 wt. % respectively. H₂ increased from 36.2 to 47.1 vol. % while CH₄ (23.2 to 14.5 vol. %) and C₂H₄ (8.7 to 5.3 vol. %) along with other hydrocarbons (0.4 to 0.3 vol. %) decreased gradually with an increase in steam/MBM. The CO increased up to 23.8 vol. % and then dropped slightly to 23.3 vol. %, while CO₂ increased slightly to 9.8 vol. % and then remained constant with further increase in steam/ MBM. The char gasification and reforming reactions are enhanced with the increase in steam/ MBM, which can be witnessed from the decrease in char, CH₄, and other H/C content. Similar trends were observed by other researchers [Ferdous *et al.*, 2001; Dalai *et al.*, 2009]. They found that H₂ and CO₂ increased

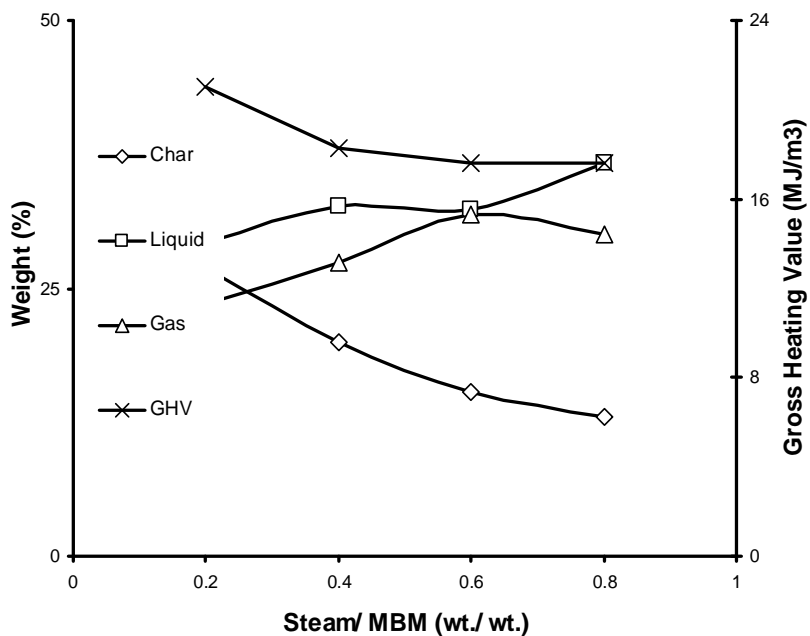


Fig. 4.14 Effect of steam/ MBM (wt/ wt) on product yield (wt. % yield) at final temperature of first stage and second stage at 850 °C, N₂ flow rate of 45 ml/min and packed bed height of 60 mm (% Difference in replicate run: Char - 0, Liquid - 0, Gas - ±1)

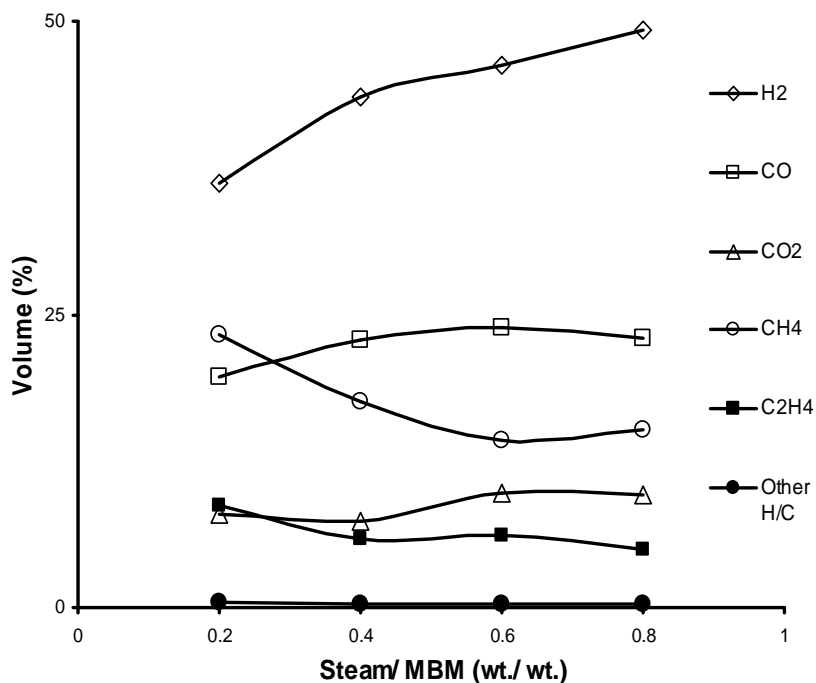


Fig. 4.15 Effect of steam/ MBM (wt/ wt) on gas composition (volume % yield (N₂ free basis)) at final temperature of first stage and second stage at 850 °C, N₂ flow rate of 45 ml/min and packed bed height of 60 mm (% Difference in replicate run: H₂ - ±4, CO - ±2, CO₂ - ±4, CH₄ - ±4, Other H/C - ±5)

while that of CH₄ and CO decreased with increased in steam flow rate during steam gasification of lignin and refuse derived fuel in fixed bed reactor system, respectively.

4.3.2.3 Effect of packed bed height

The packed bed height of the second stage was varied from 40-100 mm in increments of 20 mm by keeping the final temperatures of the first and second stages at 850 °C, N₂ flow rate at 45 ml/min, and steam/MBM (wt/ wt) at 0.8. Figs. 4.16 and 4.17 show the effect of packed bed height on product yield and gas compositions. The liquid yield decreased from 38.6 to 34.9 wt. % while that of gas increased slightly from 29.5 to 31.6 wt. %. H₂ yield increased from 45 to 48.9 vol. % and CO and CO₂ yields shifted up and down in the range of 22.5 - 22.7 and 12.4 - 10.4 vol. % respectively with increased in packed bed height from 40-100 mm. CH₄ showed a slight decrease from 14.5 to 13.3 vol. % while no significant variation observed in case of other H/C. They were constant in the range of 6.3 - 6.1 vol. %. These variations could be due to reforming of CH₄ and liquid compounds with steam and/ or CO₂ and water gas shift reactions.

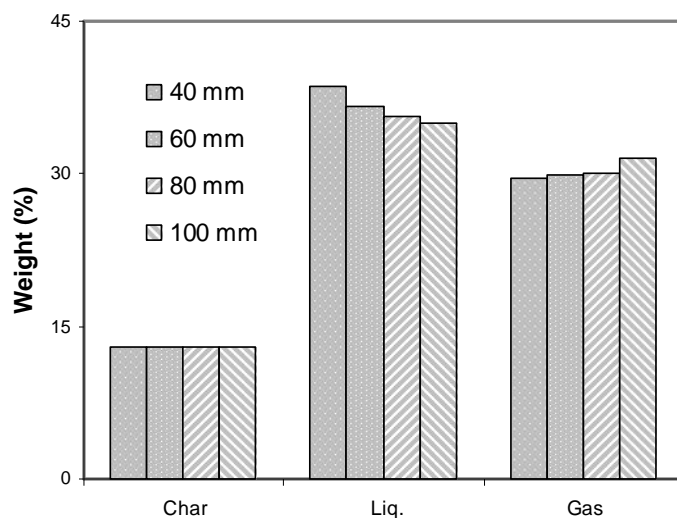


Fig. 4.16 Effect of packed bed height on product yield (wt. % yield) at steam/ MBM (wt/ wt) of 0.8, final temperature of first stage and second stage at 850 °C, and N₂ flow rate of 45 ml/min (% Difference in replicate run: Char - 0, Liquid - ±1, Gas - ±3)

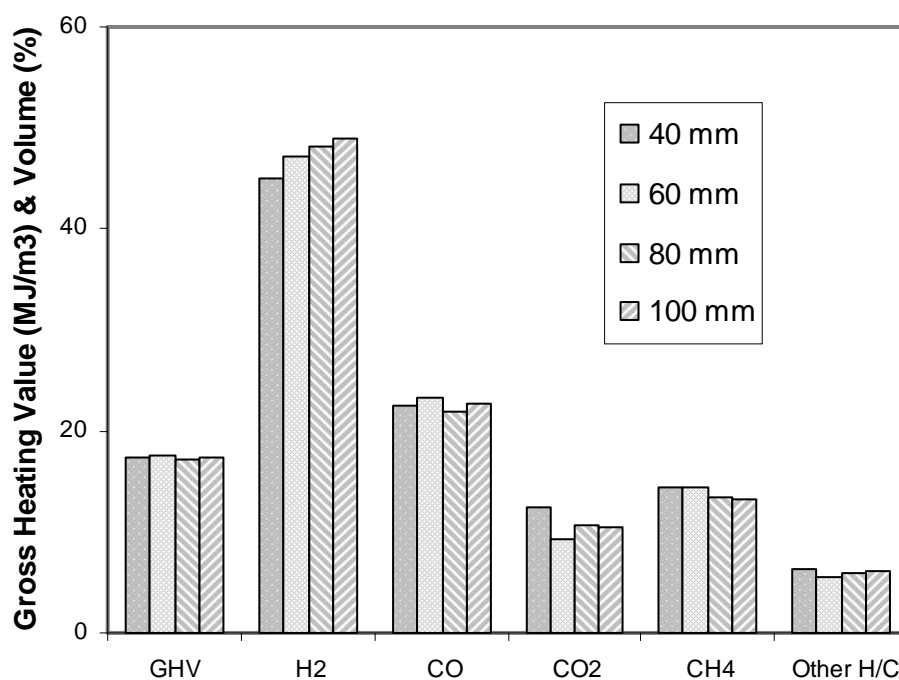


Fig. 4.17 Effect of packed bed height on gas composition (volume % yield (N₂ free basis)) and gross heating value at steam/ MBM (wt/ wt) of 0.8, final temperature of first stage and second stage at 850 °C, and N₂ flow rate of 45 ml/min (% Difference in replicate run: H₂ - ±3, CO - ±4, CO₂ - ±4, CH₄ - ±4, Other H/C - 0)

4.4 Comparison of phase I and II results

4.4.1 Single - stage operation

The comparison of phase I and II results in single stage operation is presented in Fig. 4.18. The operating conditions of phase I were: temperature of 850 °C, equivalence ratio of 0.2, and N₂ flow rate of 45 ml/min. The operating conditions of phase II were: temperature of 850 °C, steam/MBM (wt. / wt.) of 0.6, and N₂ flow rate of 45 ml/min. It is clear from the figure that the gas yield was (approximately 41 %) higher than obtained using steam, while the liquid obtained was (28 %) lower than in the case of using steam. There was a slight difference observed in case of char yield and GHV of product gases. There appears a huge difference while comparing the H₂ yield. It is way higher than in the case of using oxygen. The splitting of water molecule during gasification reactions plays a major role contributing to more H₂ in the product gas during steam gasification. CO and CO₂ contents were more during gasification using oxygen than steam, while CH₄ and other H/C contents were almost the same in both the cases.

4.4.2 Two-stage operation

The comparison of phase I and II results in two-stage operation is shown in Fig. 4.19. The operating conditions of phase I were: temperature of both the stages at 850 °C, equivalence ratio of 0.2, packed bed height of 100 mm, and N₂ flow rate of 45 ml/min. The operating conditions of phase II were: temperature of both the stages at 850 °C, steam/MBM (wt. / wt.) of 0.8, packed bed height of 100 mm, and N₂ flow rate of 45 ml/min. The trends of comparison for liquid, gas, GHV, H₂, CO, and CO₂ are same as in the case of single-stage operation. Liquid (tar + water) was almost double in case of using steam. This is due to the presence of unreacted steam in the liquid product. Gas yield was higher in the case of

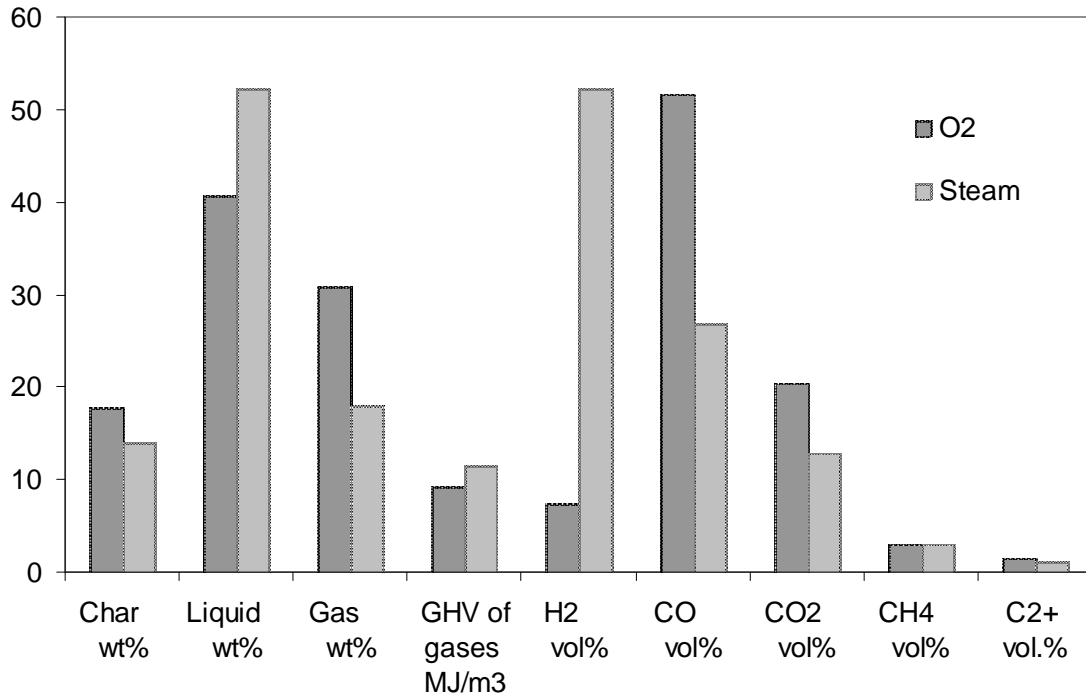


Fig. 4.18 Comparison of phase I and II results during single stage operation

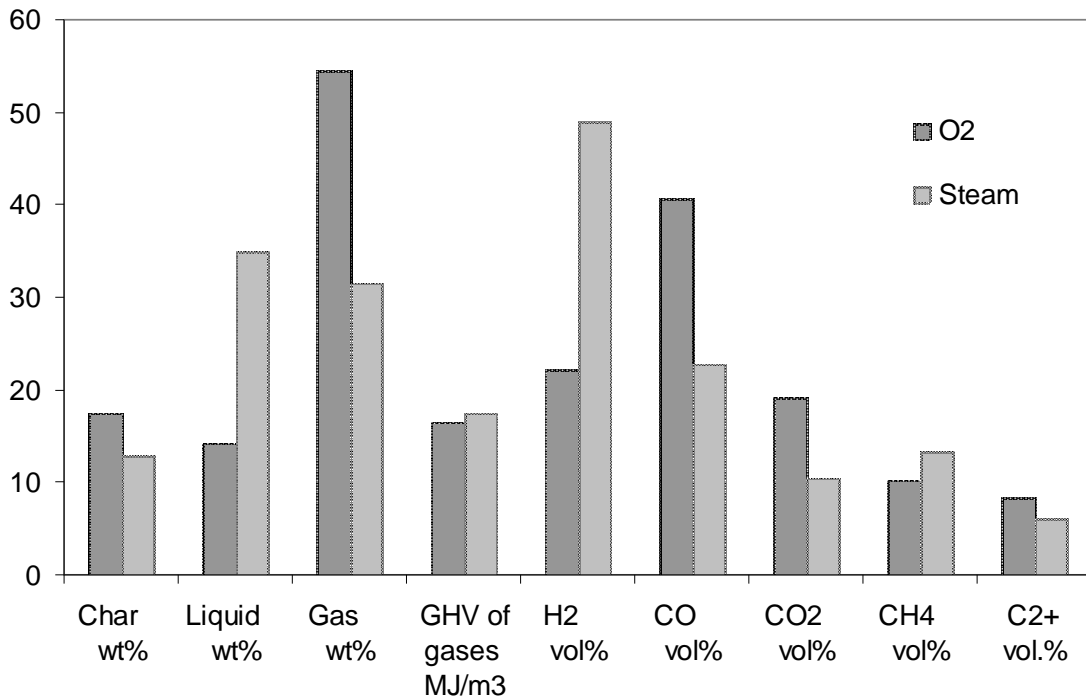


Fig. 4.19 Comparison of phase I and II results during two-stage operation

oxygen gasification, which is due to the large presence of heavier gases such as CO, CO₂ and heavier H/C. The H₂ yield was higher in steam gasification which is due to the splitting of water molecule and enhanced steam reforming reactions in second stage reactor. CH₄ content was slightly higher than gasification using oxygen, while other H/C were lower than in the case of using oxygen. This proves enhanced reforming reactions using steam as a gasifying agent.

4.5 Determination of kinetic parameters using distributed activation energy model

4.5.1 Introduction

A simple method for estimating $f(E)$ and k_0 in the distributed activation energy model was developed by Miura and Maki [1998] from his own previous work [Miura, 1995]. The new method is more accurate to estimate $f(E)$ and k_0 because it is a simple procedure and does not require a tedious differential procedure to calculate $d(V/V^*)/dt$. This model assumes that a number of parallel, irreversible and first order reactions with different activation energies occur simultaneously. All the reaction activation energies have the same frequency factor, k_0 , at the same conversion rate. The activation energy has a continuous distribution. The release of volatiles is given by:

$$V/V^* = 1 - \int_{E_s}^{\infty} f(E)dE = \int_0^{E_s} f(E)dE \quad (7)$$

Where V is the volatile evolved at temperature T , V^* is the effective volatile content, $f(E)$ is a distribution curve of the activation energy that represents the difference in the activation energies of the many first order irreversible reactions. The k_0 corresponds to the E value and a is the heating rate. Most researchers assume that $f(E)$ has a Gaussian distribution with mean activation energy E_0 . In this study, Miura's method is used to estimate $f(E)$ and k_0 of

meat and bone meal from three TGA experiments using different heating rates (10, 15, and 25 °C/ min). The calculation for E and k₀ is done using following equation [Miura and Maki, 1998].

$$\ln\left(\frac{a}{T^2}\right) = \ln\left(\frac{k_0 R}{E}\right) + 0.6075 - \frac{E}{RT} \quad (8)$$

The procedure used to estimate $f(E)$ and k_0 is summarized as follows:

1. Measure V/V* vs. T using at least three different heating rates.
2. Calculate the values of $\ln(a/T^2)$ and $1/T$ at the same V/V*.
3. Plot $\ln(a/T^2)$ and $1/T$ at the selected V/V* ratios and then determine the activation energies E from the slopes and k₀ from the intercept.
4. Plot V/V* and E and differentiate the V/V* vs. E relationship by E to obtain $f(E)$.

The following section presents results and discussion of pyrolysis of MBM to determine the kinetic parameters using a simple method in the distributed activation energy model.

4.5.2 Results and discussion

The weight loss as a function of temperature and time data was obtained for three different heating rates (10, 15, and 25 °C/ min). The plot of V/V* as a function of temperature is shown in Fig. 4.20. From this figure it can be seen that conversion of meat and bone meal increased with increase in temperature. The curve shifts to the higher temperature with increasing the heating rates. The maximum weight loss occurred between the temperature range of 500 - 700 K as seen in the Fig. 4.20. It is also observed that after 700 K, the effect of heating rate on weight loss is negligible. Moreover, there is only a marginal influence of heating rate on the overall weight loss.

Fig. 4.21 shows the graph of $\ln(a/T^2)$ and $1/T$ at the selected V/V^* ratios. The activation energy is determined as the slope of the linear fit of Fig. 4.21. Activation energies were found to increase with conversion rate as shown in Fig. 4.22. They were in the range of 60 - 246 kJ/mol for the temperature range of 496-758 K. The frequency factors, k_0 , were obtained from the intercepts of Fig. 4.21 and were 6.63×10^3 to $8.7 \times 10^{14} \text{ s}^{-1}$. Moreover, Fig. 4.23 shows the linear relationship between $\ln k_0$ and E . The graph of $f(E)$ vs. E is shown in Fig. 4.24. It shows that $f(E)$ has a maximum value of 130 kJ/mol approximately. The figure illustrates an approximate Gaussian distribution. This is also consistent with the work done by other researchers on coal and biomass [Li *et al.*, 2009; Sonobe and Worasuwanarak, 2008]. Li *et al.* [2009] used distributed activation energy model to calculate kinetic parameters for pyrolysis of two coal and corn stalk skins samples. The temperature range was 40 to 900 °C for corn stalk sample while it was 40 to 1200 °C for coal samples. The E value was found in the range of 100-486 kJ/mol with corresponding k_0 of 2.94×10^8 to $4.2 \times 10^{25} \text{ s}^{-1}$ and 100-462 kJ/mol with corresponding k_0 of 4.42×10^5 to $1.71 \times 10^{24} \text{ s}^{-1}$ for Datong bituminous and Jindongnon lean coal respectively. The values of E and k_0 for corn stalk skins were in the range of 62-169 kJ/mol and 4.9×10^4 - $3.22 \times 10^{11} \text{ s}^{-1}$ respectively. Sonobe and Worasuwanarak [2008] used distributed activation energy model to calculate the kinetic parameters for the pyrolysis of rice straw, rice husk, and corn cob. They found k_0 increased from 10^{11} to an order of 10^{18} s^{-1} where E increased from 120 to 250 kJ/mol for the final pyrolysis temperature of 900 °C.

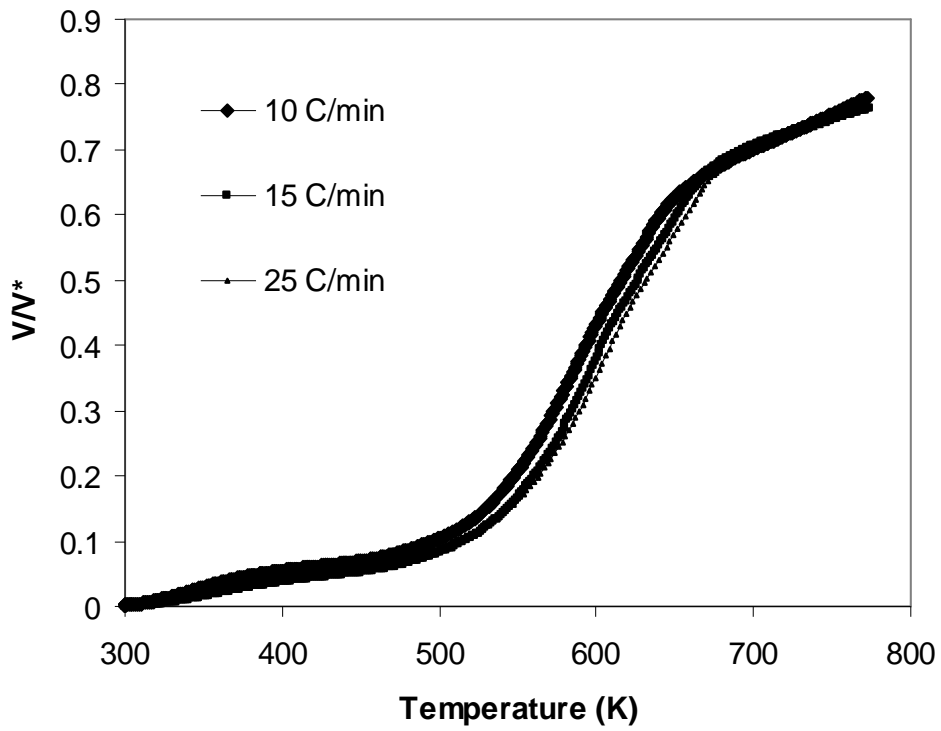


Fig. 4.20 Effect of temperature on V/V^* during pyrolysis of MBM in thermogravimetric analyzer for three different heating rates

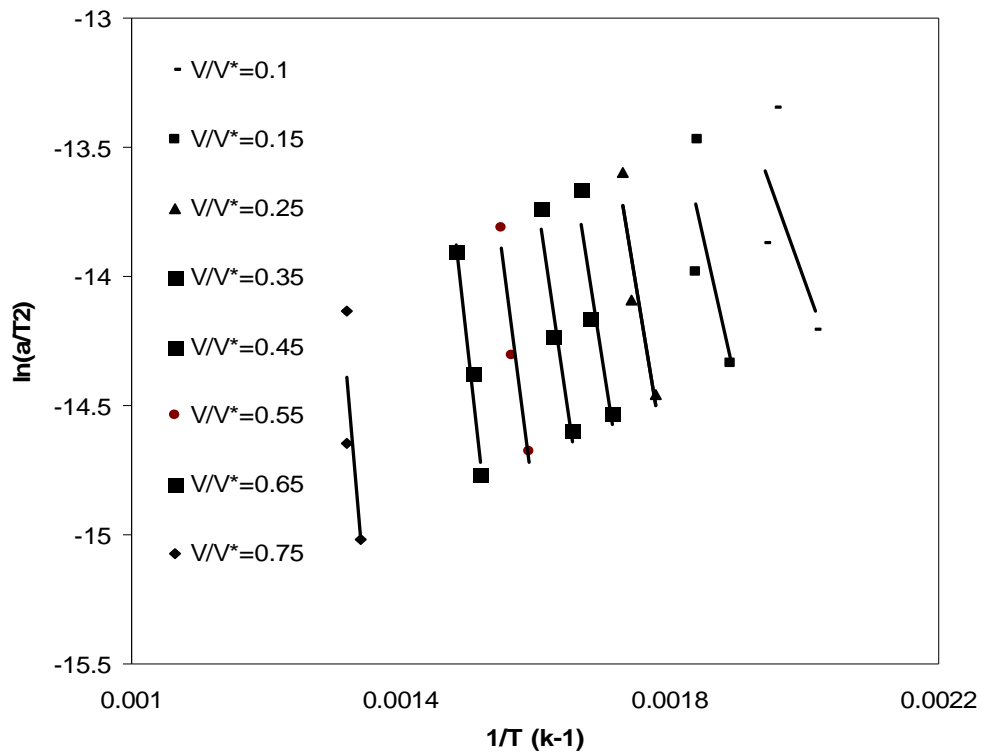


Fig. 4.21 $\ln(a/T^2)$ vs. $1/T$ at the selected V/V^* ratios

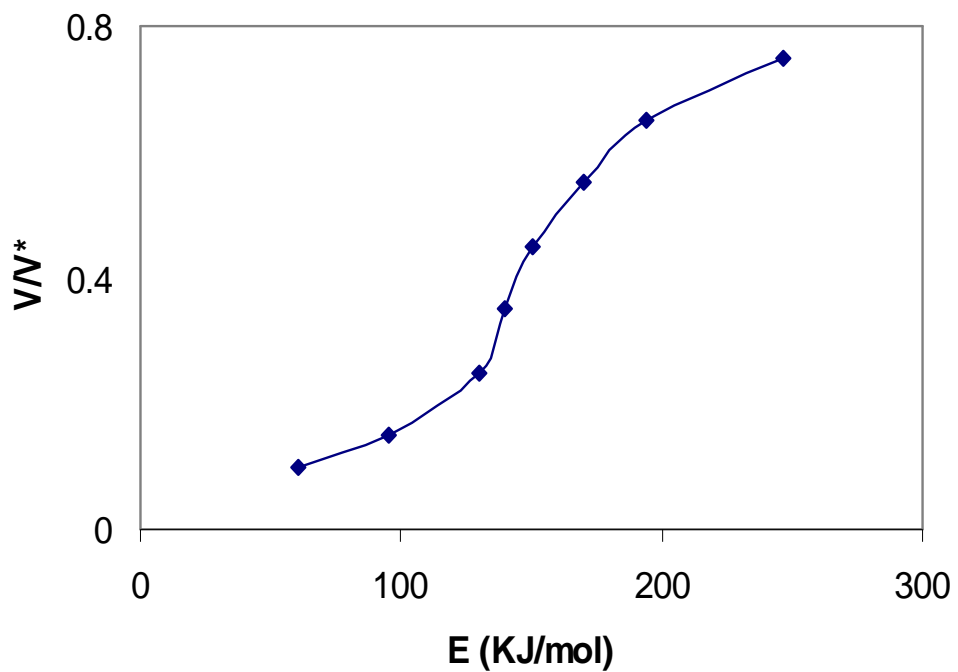


Fig. 4.22 V/V^* vs. E relationship

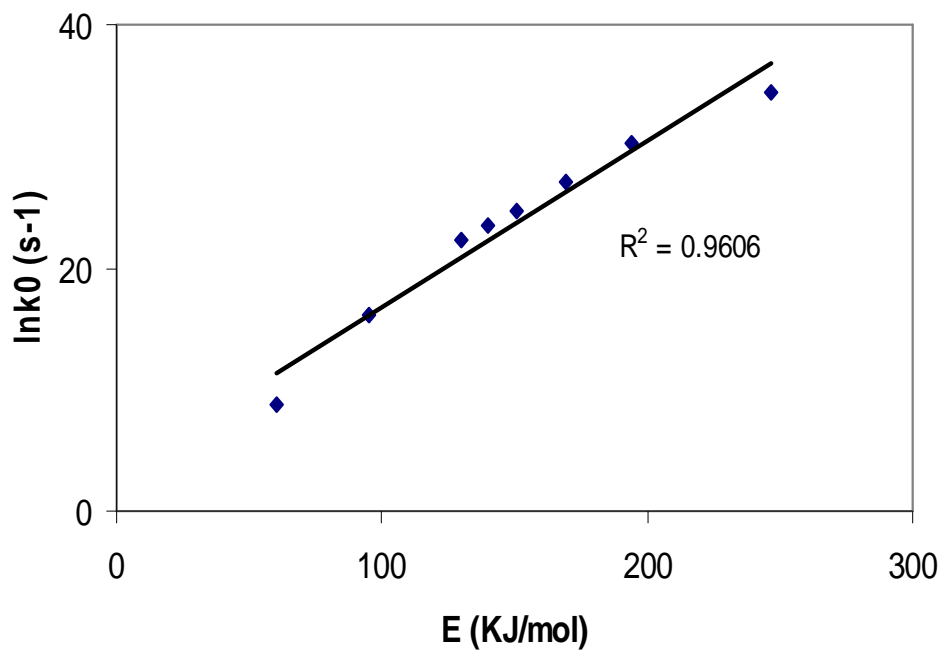


Fig. 4.23 $\ln k_0$ vs. E relationship

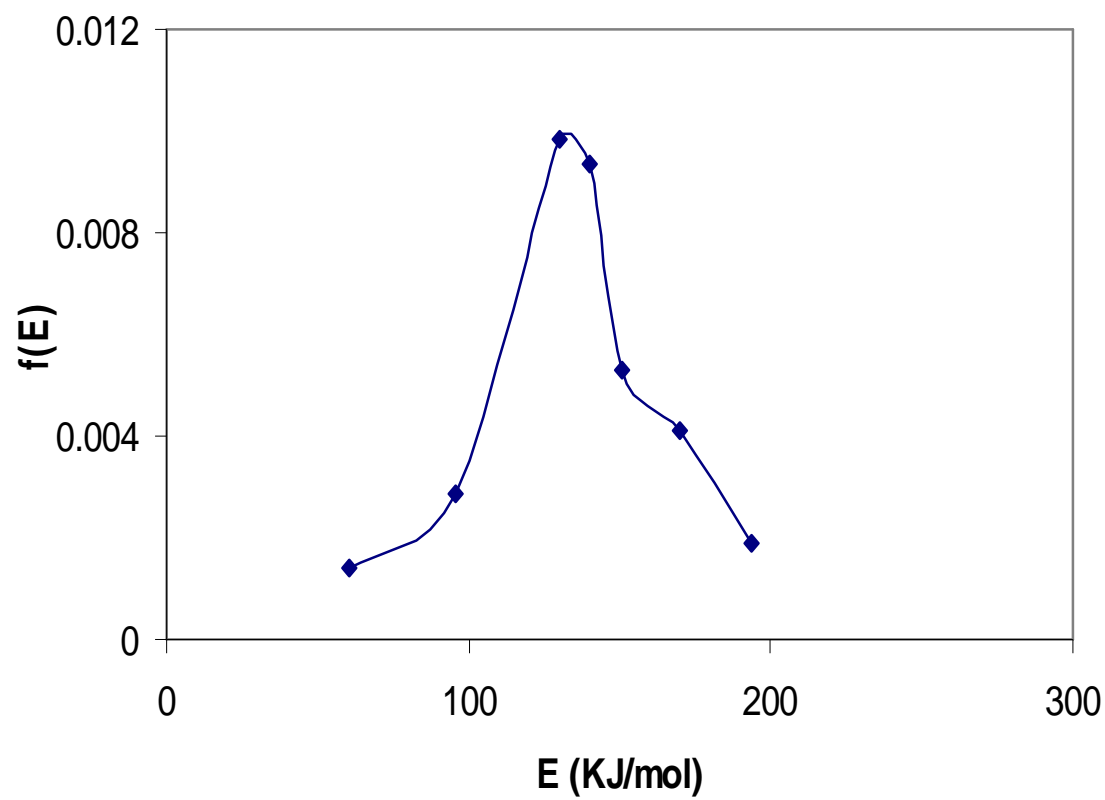


Fig. 4.24 $f(E)$ vs. E relationship

Chapter 5

CONCLUSIONS AND RECOMMENDATIONS

5.1 Conclusions

In general, it has been concluded that meat and bone meal (MBM) can be effectively gasified using pure oxygen and steam as the gasifying agents.

The following conclusions were made regarding gasification of meat and bone meal using pure oxygen:

1. Higher temperature of 850 °C of both the stages was found to be favorable for higher hydrogen/syngas production within the temperature range (650 - 850 °C) studied.
2. In comparison to single stage process, two- stage process was proved to be effective in increasing the H₂ yield from 7.3 to 22.3 vol. % and the gas yield from 30.8 to 54.6 wt. %. At the same time, the tar yield was reduced from 40.7 to 14.2 wt. %.
3. The equivalence ratio (ER) of 0.2 was found to be optimal to yield maximum H₂ production of 21.2 vol. % at the final temperature of first stage and second stage temperature of 850 °C, N₂ flow rate of 45 ml/min and packed bed height of second stage at 60 mm.
4. Packed bed height was found to have a least impact. The tar yield decreased slightly from 18.6 to 14.2 wt. % while gas yield increased from 50.6 to 54.6 wt. % with an increase in packed bed height of second stage from 40 to 100 mm. There was no significant variation observed in gas compositions.

The following conclusions were made regarding gasification of meat and bone meal using steam:

1. Higher temperature of 850 °C of both stages was found to be favorable for higher gas yield and hydrogen production within the temperature range studied (650 – 850 °C).
2. Two-stage process was found to be effective to reduce the liquid yield and to increase gas yield.
3. With increased in steam/ MBM (wt/ wt) ratio, hydrogen (36.2 to 49.2 vol. %) and gas (29.2 to 36.7 wt. %) yields were increased while char (27 to 13 wt. %), CH₄ (23.2 to 15.1 vol. %) and other H/C yields decreased.
4. With increased in packed bed height from 40 to 100 mm, gas (29.5 to 31.6 wt. %) and hydrogen (45 to 49.2 vol. %) yields increased. There was no significant variation observed in case of heavier hydrocarbons.

The following conclusions were derived from the comparison of phase I and II results during two-stage operation at the optimum conditions.

1. No major difference observed in case of char yields and GHV in both the phases, while liquid yield (phase I: 14.2 wt. %; phase II: 34.9 wt. %) was almost double in the case of steam gasification.
2. Oxygen was found to yield more gas (phase I: 54.6 wt. %; phase II: 31.6 wt. %) than steam due to high amount of CO and CO₂ present in the product gas.
3. Steam was found an effective oxidant over oxygen to increase the H₂ (phase I: 22.3 vol. %; phase II: 48.9 vol. %) yield and to reduce the heavier H/C in the product gas.

The following conclusions were made regarding the kinetic analysis for pyrolysis of meat and bone meal:

1. Simple method of distributed activation energy model fitted experimental results of pyrolysis of meat and bone meal using a thermogravimetric analyzer. Experiments also showed that $f(E)$ vs. E have an approximate Gaussian distribution.
2. The activation energies were in the range of 60 - 246 kJ/mol for the temperature range of 496 - 758 K with corresponding frequency factors of 6.63×10^3 to 8.7×10^{14} s⁻¹.

5.2 Recommendations

The following important recommendations were made for further studies.

1. In the present work, the range of parameters was carefully chosen based on the literature review and experimental set up limitations. It is recommended to further expand the range.
2. Continuous systems such as fluidized bed reactors are always of an industrial interest. It is recommended to test gasification parameters and pursue detail kinetic modeling of MBM gasification using a fluidized bed reactor system.
3. Experiments were carried out without statistical design. It is also recommended to pursue experimental design of the important parameters to optimize the operating conditions in both continuous and semi-batch systems.
4. All experiments were carried out in non-catalytic systems. Selective catalyst can help to reduce tar content and enhance reforming reactions. It is advisable to use commercial or synthesized catalysts in the gasification process.

5. Combination of both oxygen and steam has been reported effective in few gasification processes. It is also an important parameter to consider in future studies.
6. Detail cost estimation and feasibility study of MBM gasification is to be carried out for industrial applicability.

Chapter 6

REFERENCES

Aguado, R., M. Olazar, B. Gaisan, R. Prieto, and J. Bilbao, "Kinetic Study of Polyolefin Pyrolysis in a Conical Spouted Bed Reactor", *Ind. Eng. Chem. Res.* 2002, 41, 4559-4566

Ayllon, M., G. Gea, M.B. Murillo, J.L. Sanchez, and J. Arauzo, "Kinetic study of meat and bone meal pyrolysis: an evaluation and comparison of different possible kinetic models", *Journal of Applied Pyrolysis* 74 (2005), 445-453.

Ayllon, M., M. Aznar, J.L. Sanchez, G. Gea, and J. Arauzo, "Influence of temperature and heating rate on the fixed bed pyrolysis of meat and bone meal", *Chemical Engineering Journal* 121 (2006), 85-96.

Bradley R., "Bovine Spongiform Encephalopathy (Bse): The Current Situation and Research", *Eur Journal of Epidemiology* 7 (1991), 532-44.

Bridgwater, A.V., "The technical and economic feasibility of biomass gasification for power generation", *Fuel* 74 (1995), 631-653.

Bruce, M.E., R.G. Will, J.W. Ironside, I. McConnell, D. Drummond, A. Suttie, L. McCardle, A. Chree, J. Hope, C. Birkett, S.N. Cousens, H. Fraser, and C.J. Bostock, "Transmissionstomiceindicate that 'newvariant' CJD is caused by the BSE agent", *Nature* 389 (1997), 498-501.

Chaala, A., and C. Roy, "Recycling of Meat and Bone Meal Animal Feed by Vacuum Pyrolysis", *Environ. Sci. Technol.* 37 (2003), 4517-22.

Chalus T. and I. Peutz BSE: the European regulatory context. *Euro Surveill.* (2000); 5(10):pii=2. Available online:
<http://www.eurosurveillance.org/ViewArticle.aspx?ArticleId=2>, last accessed on July 31 (2009).

Channiwala, S.A. and P.P. Parikh, "A Unified Correlation for Estimating HHV of solid, liquid and gaseous fuels", *Fuel* 81 (2002), 1051-1063.

Cipriani P., D.P. Filippis, and F.J. Pochetti, "Solid waste gasification: Energy recovery from polyethylene biomass mixtures" *Solid Waste Tech. Mang.* 25 (1998), 77-81.

Conesa, J.A., A. Fullana, and R. Font, "Thermal decomposition of meat and bone meal", *Journal of Anal. Appl. Pyrolysis* 70 (2003), 619-630.

Cyr, M. and C. Ludmann, "Low risk meat and bone meal (MBM) bottom ash in mortars as sand replacement", *Cement and Concrete Research* 36 (2006), 469-480.

Dalai, A.K., N. Batta, I. Eswaramoorthi, and G.J. Schoenau, "Gasification of refuse derived fuel in a fixed bed reactor for syngas production", *Waste Management* 29 (2009), 252-258.

Della Rocca, P.A., E.G. Cerrella, P.R. Bonelli, and A.L. Cukierman, “Pyrolysis of hardwoods residues: on kinetics and chars characterization”, *Biomass and Bioenergy* 16 (1999) 79-88.

Demirbas, M.F., M. Balat, and H. Balat, “Potential contribution of biomass to the sustainable energy development”, *Energy Conversion and Management* 50 (2009) 1746–1760.

Devi L., K.J. Ptasiński, F.J.J.G. Janssen, S.V.B. Van Paasen, P.C.A. Bergman, and J.H.A. Kiel, “Catalytic decomposition of biomass tars: use of dolomite and untreated olivine”, *Renewable Energy* 30 (2005), 565-87.

Directorate General for Health and Consumers, “European Commission decides new measures on BSE: exceptional events call for an exceptional response”, last accessed on July 31 (2009) website: http://ec.europa.eu/dgs/health_consumer/library/press/press90_en.html.

Energy Information Administration (EIA), *International Energy Outlook* (May, 2009), last assessed on July 31 (2009) website: <http://www.eia.doe.gov/oiaf/ieo/>

Fedorowicz, M.E., S.F. Miller, and B.G. Miller, “Biomass Gasification as a Means of Carcass and Specified Risk Materials Disposal and Energy Production in the Beef Rendering and Meatpacking Industries”, *Energy & Fuels* 21 (2007), 3225-32.

Ferdous, D., A.K. Dalai, S.K. Bej, and R.W. Thring, "Production of H₂ and medium heating value gas via steam gasification of lignins in fixed-bed reactors", *The Canadian Journal of Chemical Engineering* 79 (2001), 913-922.

Franco, C., F. Pinto, I. Gulyurtlu, and I. Cabrita, "The study of reactions influencing the biomass steam gasification process", *Fuel* 82 (2003), 835-842.

Freeman, E.S. and B. Carroll, "The application of thermoanalytical techniques to reaction kinetics. The thermogravimetric evaluation of the kinetics of the decomposition of calcium oxalate monohydrate", *Journal of Physical Chemistry* 62 (1958), 394-397.

Fryda, L., K. Panopoulos, P. Vourliotis, E. Pavlidou, and E. Kakaras, "Experimental investigation of fluidised bed co-combustion of meat and bone meal with coals and olive bagasse", *Fuel* 85 (2006), 1685-99.

Garcia-Ibanez, P., M. Sanchez, and A. Cabanillas, "Thermogravimetric analysis of olive-oil residue in air atmosphere", *Fuel Processing Technology* 87 (2006), 103-107.

Garcia, R.A., K.A. Rosentrater, and R.A. Flores, "Characteristics of North American Meat and Bone Meal Relevant To the Development of Non-Feed Applications", *American Society of Agricultural and Biological Engineers*, 22(5) (2006), 729-736.

Gulyurtlu, I., D. Boavida, P. Abelha, M.H. Lopes, and I. Cabrita, “Co-combustion of coal and meat and bone meal”, *Fuel* 84 (2005), 2137-2148.

Han, J. and H. Kim, “The reduction and control technology of tar during biomass gasification/ pyrolysis: An overview”, *Renewable and Sustainable Energy Reviews* (2006), doi:10.1016/j.rser.2006.07.015

Higman, C. and M. Van der Burgt, “Gasification, second edition”, Gulf Professional Publishing (2008).

Li, Z., C. Liu, Z. Chen, J. Qian, W. Zhao, and Q. Zhu, “Analysis of coals and biomass pyrolysis using the distributed activation energy model”, *Bioresource Technology*, 100 (2009), 948-952.

Lv, P.M., Z.H. Xiong, J. Chang, C.Z. Wu, Y. Chen, and J.X. Zhu, “An experimental study on biomass air–steam gasification in a fluidized bed”, *Bioresource Technology* 95 (2004), 95-101.

Mansaray, K.G., A.E. Ghaly, A.M. Al-Taweel, F. Hamdullahpur, and V.I. Ugursal, “Air gasification of rice husk in a dual distributor type fluidized bed gasifier”, *Biomass and Bioenergy* 17 (1999), 315-332.

Mansaray, K.G. and A.E. Ghaly, “Determination of kinetic parameters of rice husks in oxygen using thermogravimetric analysis”, *Biomass and Bioenergy* 17 (1999), 19-31.

Manya, J.J., J.L. Sa´nchez, J. Abrego, A. Gonzalo, and J. Arauzo, “Influence of gas residence time and air ratio on the air gasification of dried sewage sludge in a bubbling fluidised bed”, *Fuel* 85 (2006), 2027–2033.

Miura, K., “A New and Simple Method to Estimate $f(E)$ and $k_0(E)$ in the Distributed Activation Energy Model from Three Sets of Experimental Data”, *Energy & Fuels* 9 (1995), 302-307.

Miura, K. and T. Maki, “A Simple Method for Estimating $f(E)$ and $k_0(E)$ in the Distributed Activation Energy Model”, *Energy & Fuels* 12 (1998), 864-869.

Narvaez, I., A. Orio, M.P. Aznar, and J. Corella, “Biomass Gasification with Air in an Atmospheric Bubbling Fluidized Bed. Effect of Six Operational Variables on the Quality of the Produced Raw Gas”, *Ind. Eng. Chem. Res.* 35 (1996), 2110-2120.

Perry, H.R. and D.W. Green, “Perry’s Chemical Engineering Handbook, 7th Edition”, McGraw Hill (1997).

Pilawska, M., J. Baron, W. Zukowski, and S. Kandefer, “The Use of AB FBC for the Utilization of Raw Animal Wastes”, *The Seventh Asia-Pacific International Symposium on Combustion and Energy Utilization, Hong Kong SAR, proceedings 15-17 December 2004.*

Rodehutsord M., H.J. Abel, W. Friedt, C. Wenk, G. Flachowsky, H.J. Ahlgrimm, B. Johnke, R. Kuhl, and G. Breves, “Review article consequences of the ban of by-products from

terrestrial animals in livestock feeding in Germany and the European Union: Alternatives, nutrient and energy cycles, plant production, and economic aspects”, *Arch. Anim. Nutr.* 56 (2002) 67-91.

Skytte, K., P. Meibom, and T.C. Henriksen, “Electricity from biomass in the European union—with or without biomass import”, *Biomass and Bioenergy* 30 (2006) 385–392.

Sonobe, T. and N. Worasuwannarak, “Kinetic analyses of biomass pyrolysis using the distributed activation energy model”, *Fuel* 87 (2008), 414-421.

Taylor, D.M., K. Fernie, and I. McConnell, “Inactivation of the 22A strain of scrapie agent by autoclaving in sodium hydroxide“, *Veterinary Microbiology* 58 (1997), 87-91.

Timilsina, G.R., “Atmospheric stabilization of CO₂ emissions: Near-term reductions and absolute versus intensity-based targets”, *Energy Policy* 36 (2008) 1927–1936.

Wei, L., S. Xu, L. Zhang, C. Liu, H. Zhu, and S. Liu, “Steam gasification of biomass for hydrogen-rich gas in a free-fall reactor”, *International Journal of Hydrogen Energy* 32 (2007), 24-31.

Wrobel, J and P. Wright, “Calorific values and Relative densities, Calculations from Composition”, *Technical Monograph Series Communication* 1080 (1978).

Xiao, R., B. Jin, H. Zhou, Z. Zhong, and M. Zhang, “Air gasification of polypropylene plastic waste in fluidized bed gasifier”, *Energy Conversion and Management* 48 (2007), 778-786.

Zhu, X. and R. Venderbosch, “A correlation between stoichiometrical ratio of fuel and its higher heating value”, *Fuel* 84 (2005) 1007–1010.

APPENDIX A: Calibration of mass flow meters, syringe pump, and GCs HP 5880 and 5890.

A.1 Calibration of mass flow meters (Aalborg model GFM17)

Two different mass flow meters were used in the experiments with different ranges. The one used for N₂ gas had a range of 0-200 ml/min while the one used for O₂ gas had a range of 0-20 ml/min. The calibration curves for both are given below.

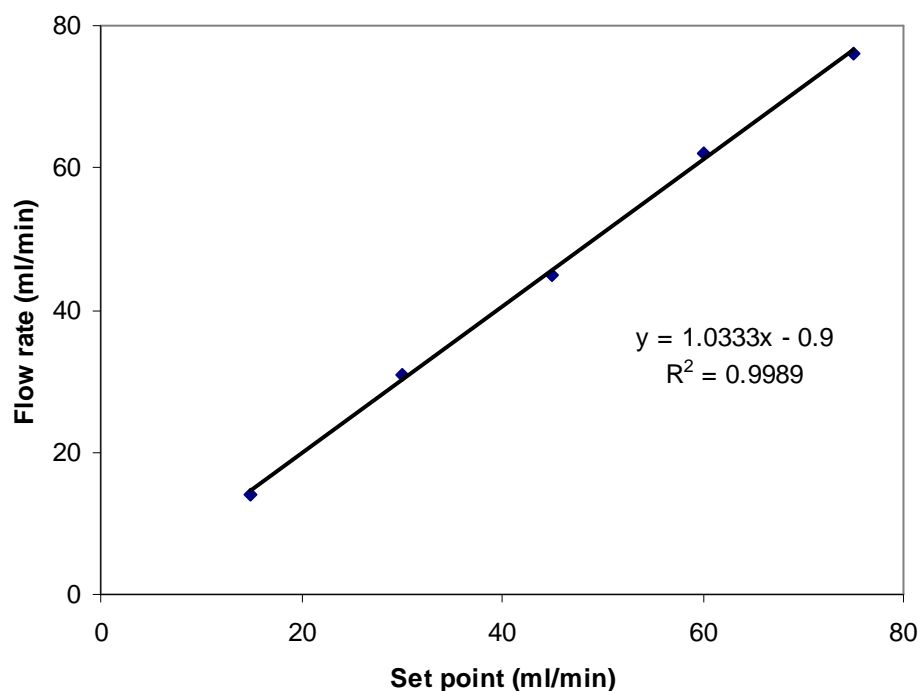


Fig. A.1 Calibration of mass flow meter (0-200 ml/min)

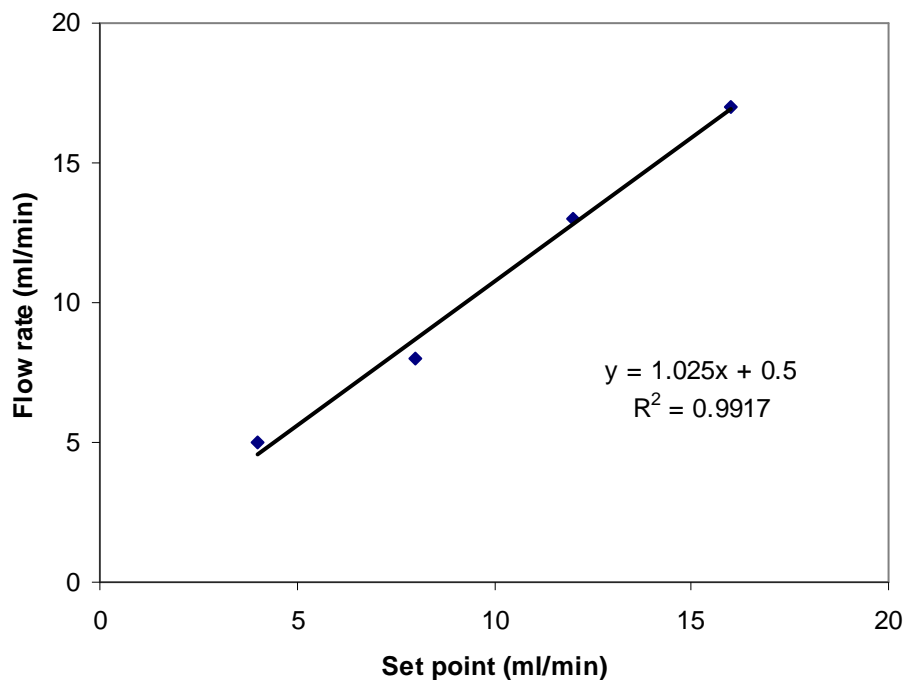


Fig. A.2 Calibration of mass flow meter (0-20 ml/min)

A.2 Calibration of syringe pump (Kent Scientific, Genie Plus Model, USA)

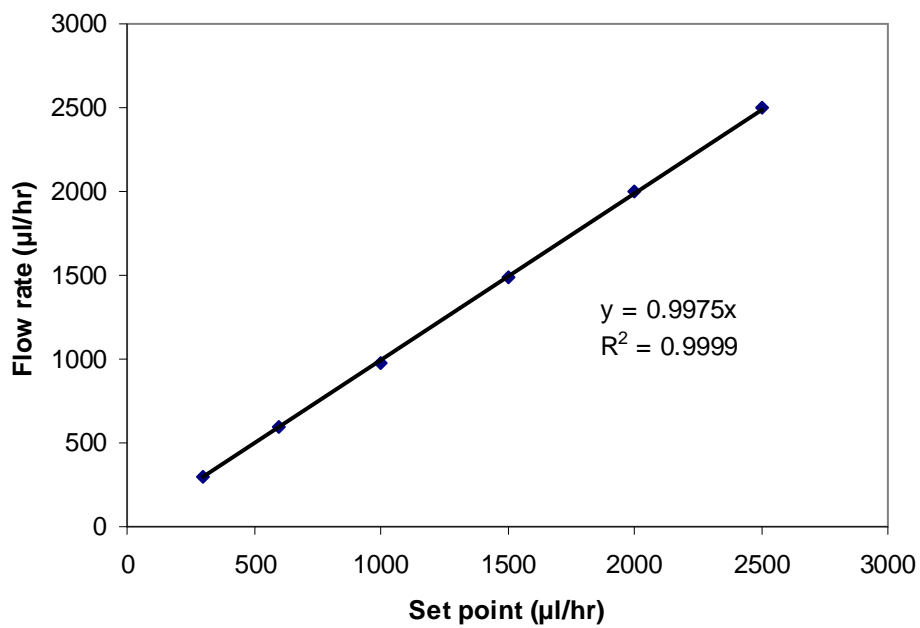


Fig. A.3 Calibration of mass flow meter

A.3 Calibration of GCs HP 5880 and 5890

The calibration of GCs HP 5880 and 5890 was carried out using standard gas mixtures. The information related to GCs program is already explained in detail in section 3.3.

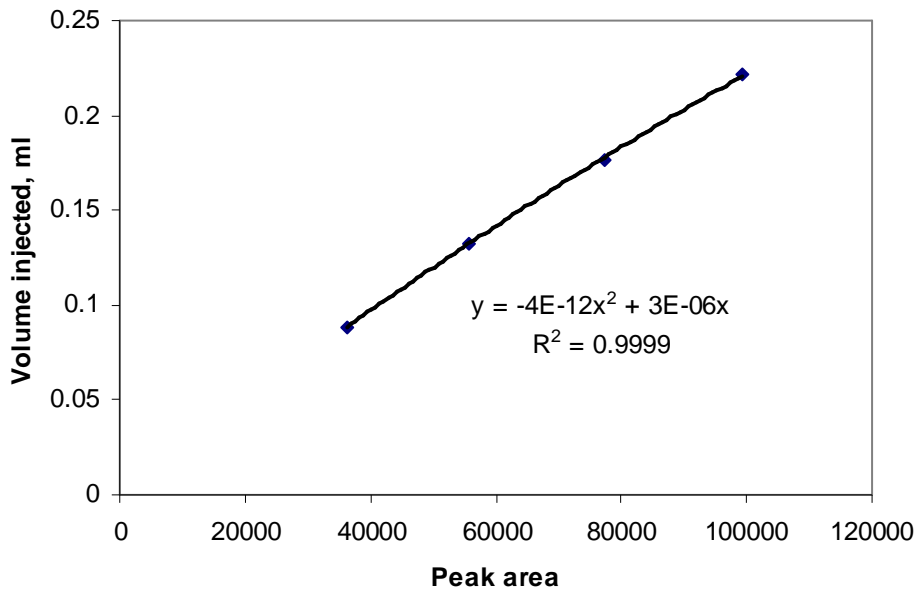


Fig. A.4 Calibration curve of H₂

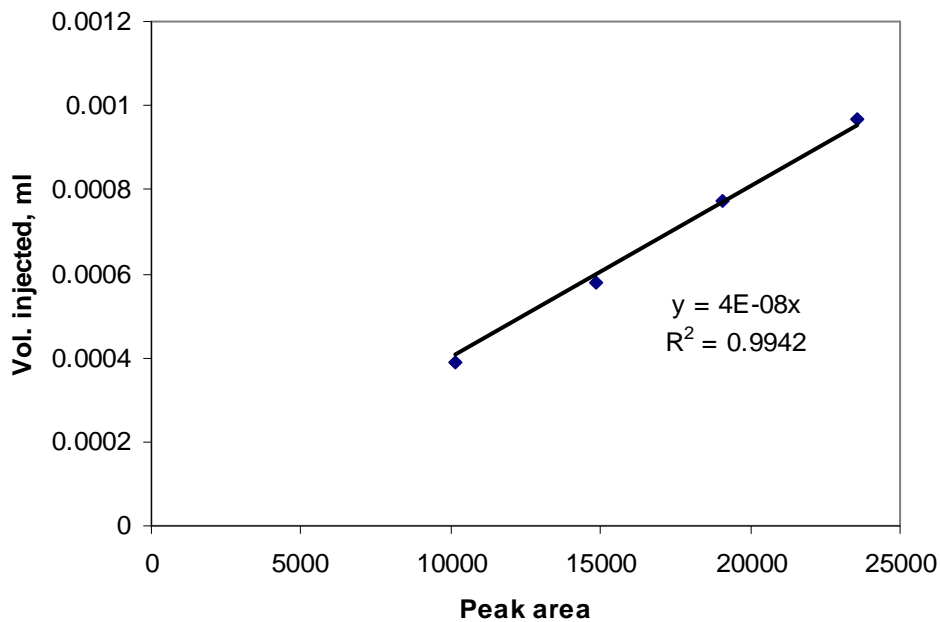


Fig. A.5 Calibration curve of CO

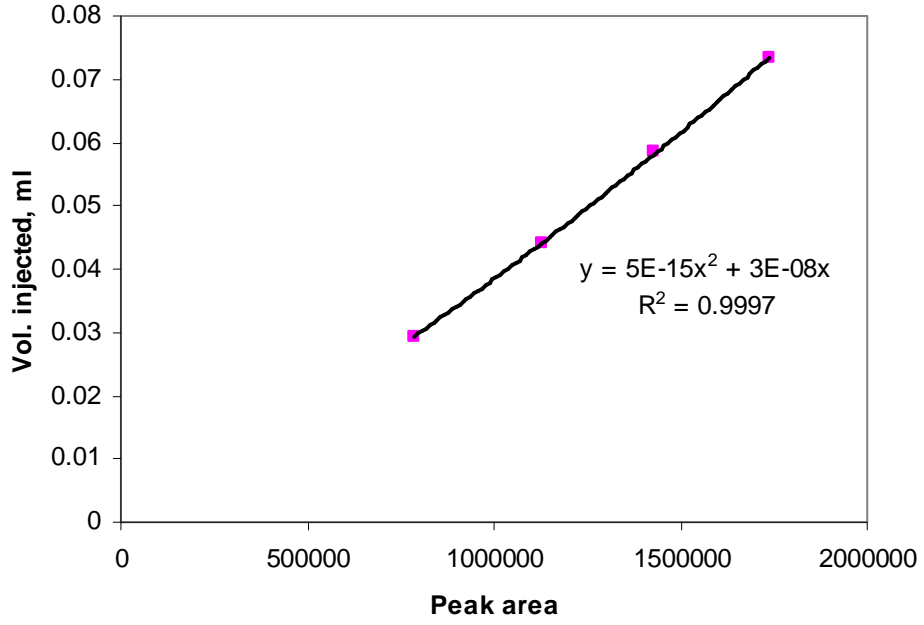


Fig. A.6 Calibration curve of CO₂

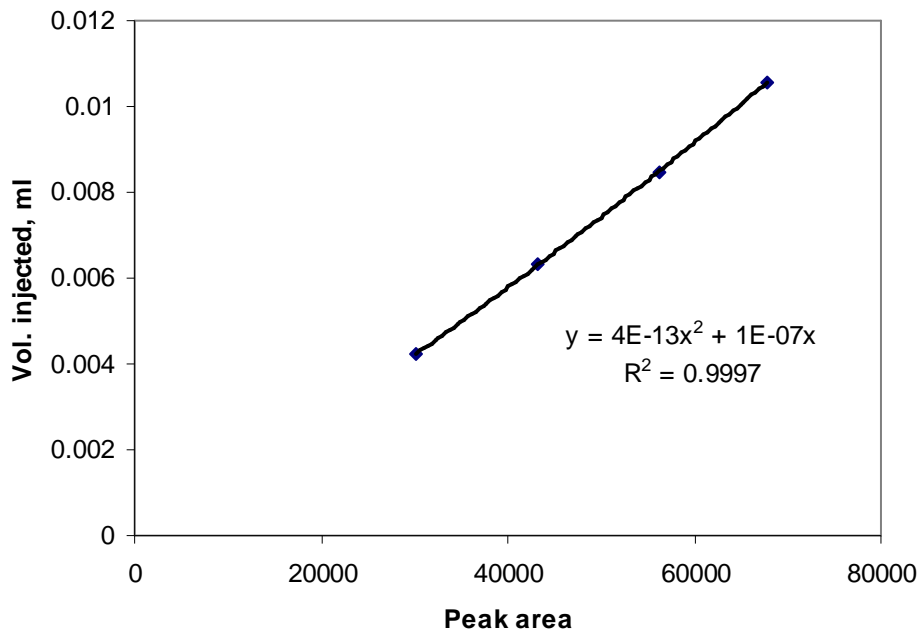


Fig. A.7 Calibration curve of CH₄

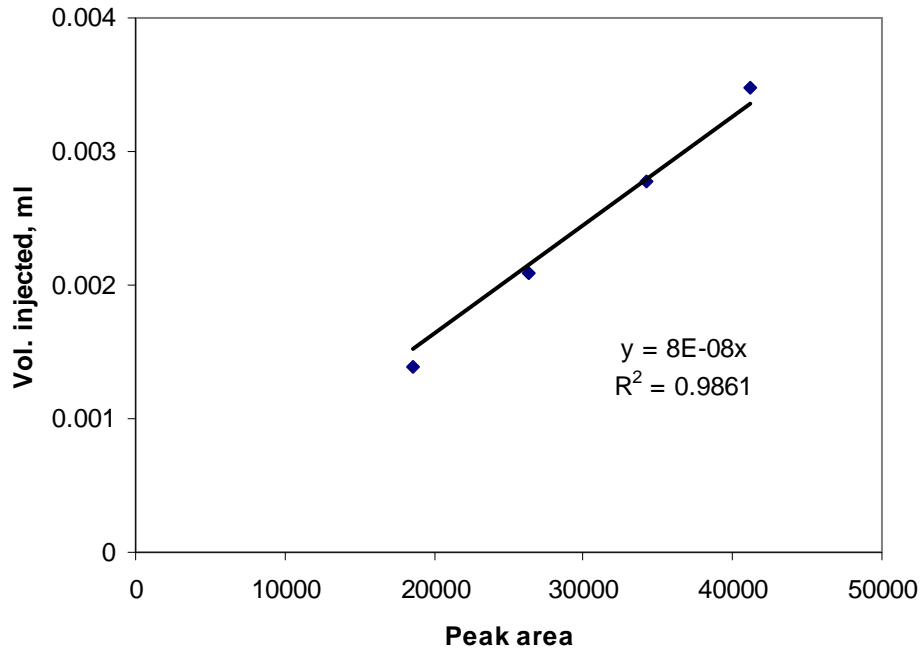


Fig. A.8 Calibration curve of C₂H₄

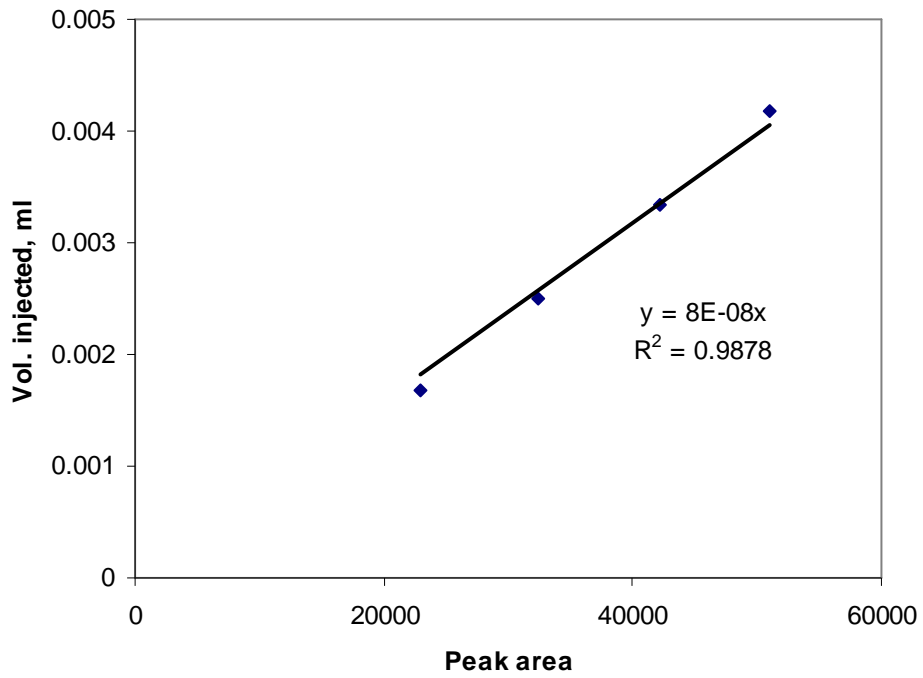


Fig. A.9 Calibration curve of C₂H₆

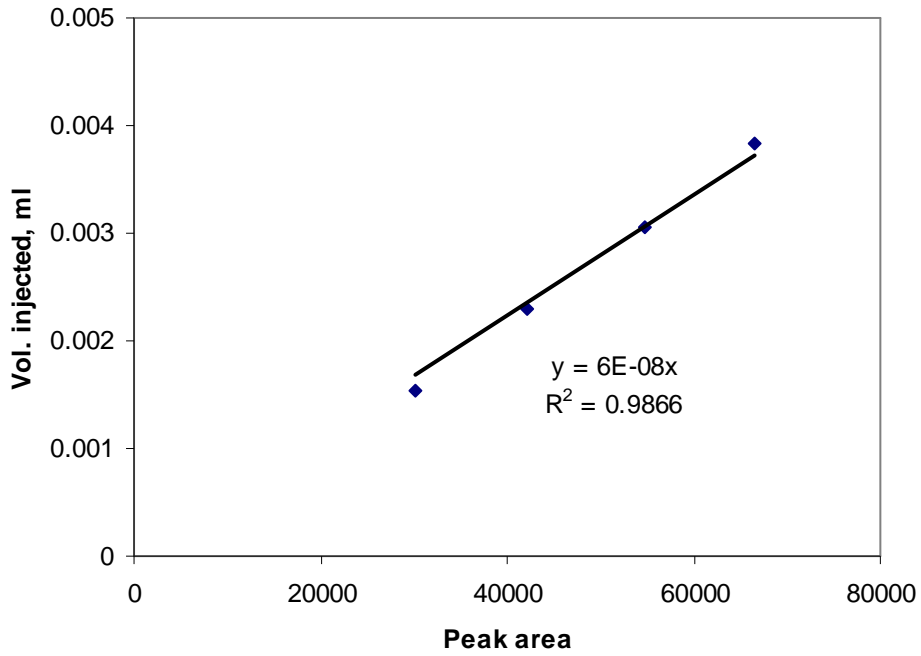


Fig. A.10 Calibration curve of C₃H₆

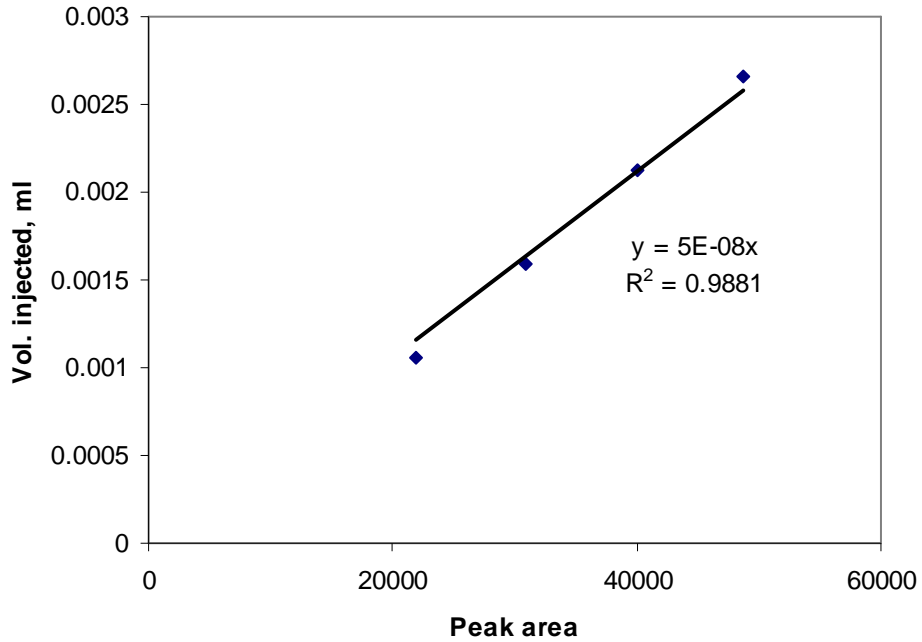


Fig. A.11 Calibration curve of C₃H₈

APPENDIX B: Sample calculation for mass balance and calorific value of product gas

B1: Gasification of MBM using steam

The sample calculation presented here is for the effect of temperature in two-stage operation.

The overall mass balance was in the range of 80 to 90 %, which is due to the presence of some unknown gases in the product gas and mass loss during experimentation.

Experimental conditions:

MBM sample: 2 g

Total amount of steam supplied: 0.99 g

Temperature of 1st stage: 850 °C, Temperature of 2nd stage: 650 °C

Steam/ MBM (wt. / wt.): 0.6

Packed bed height: 60 mm

N₂ flow rate: 45 ml/min

Observations:

Weight of reactor before the reaction (including MBM): 247.6 g

Weight of reactor after the reaction: 246.05

Weight of char left: $2 - (247.6 - 246.05) = 0.45$ g

Weight of condenser before the reaction: 135.32 g

Weight of condenser after the reaction: 136.49 g

Weight of liquid (tar + water) collected: $136.49 - 135.32 = 1.17$ g

Total volume of gas collected (including N₂): 4085 ml

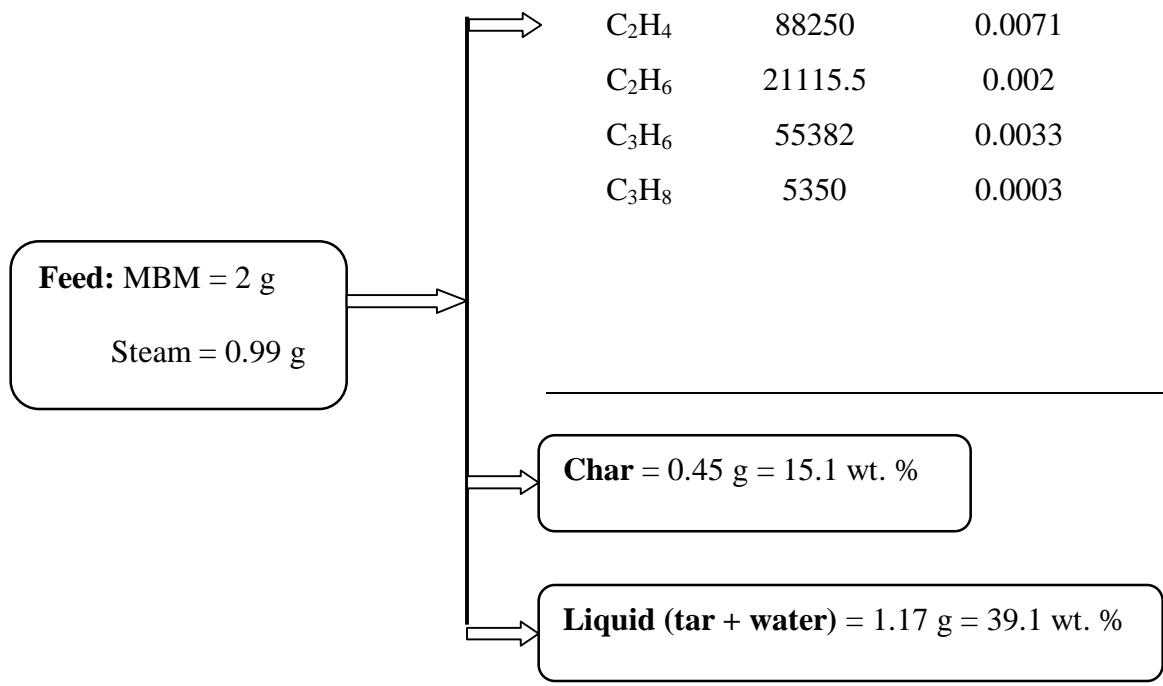
Total volume of product gases produced (excluding N₂): 1160 ml

Volume of gas injected into GCs was 0.5 ml. Table B1 shows the calculation for gas compositions and weight of product gas.

Table B1 Calculation for gas compositions and weight of product gas

Component	Peak area	Vol. in injected sample (0.5 ml) ml	Total vol. in gas collected ml	Total moles in gas collected gmole	Weight g
H ₂	19402	0.0567	463	0.019	0.039
CO	837408	0.033	273	0.012	0.32
CO ₂	461105	0.014	121	0.005	0.23
CH ₄	66975.5	0.011	90	0.0035	0.056
C ₂ H ₄	88250	0.0071	58	0.0025	0.07
C ₂ H ₆	21115.5	0.002	16.3	0.0007	0.021
C ₃ H ₆	55382	0.0033	27.2	0.0011	0.0462
C ₃ H ₈	5350	0.0003	2.5	0.0001	0.0044
			Total vol. =		Total gas wt.
			1051 ml		= 0.8 g
					= 26.8 wt. %

80



B2: Calculation for finding the calorific value of product gas:

Calorific value of the product gas was calculated at 15 °C temperature and atmospheric pressure. The ideal gas calorific value is given by [Wrobel and Wirght, 1978]

$$CV = x_1*CV_1 + x_2*CV_2 + \dots + x_n*CV_n$$

Where, x_1, x_2, \dots represent vol. fractions and CV_1, CV_2, \dots represent calorific values of ideal gases. The sample calculation to calculate calorific value of product gas is shown in Table B2.

Table B2 Calculation for calorific value of product gas

Component	Calorific value at 15 °C and atm. Pressure MJ/m ³	Total volume in product gas ml	Volume % (Based on actual vol. collected)	Calorific value MJ/m ³
H ₂	12.1	463	39.9	4.82
CO	11.97	273	23.5	2.81
CH ₄	37.71	90	7.8	3.0
C ₂ H ₄	59.72	58	5.0	3.0
C ₂ H ₆	66.07	16.3	1.4	0.93
C ₃ H ₆	87.09	27.2	2.3	2.0
C ₃ H ₈	93.94	2.5	0.23	0.22
			Total	16.8

Appendix C: Experimental results with replicate runs

Phase I: Gasification of MBM using oxygen in single stage and two-stage operations

Table C1 Effect of temperature during single-stage operation

MBM g	O ₂ g	T ₁ °C	Char wt. %	Tar wt. %	Gas wt. %	Calorific value of product gas MJ/m ³	H ₂ vol.%	CO vol.%	CO ₂ vol.%	CH ₄ vol.%	C ₂ H ₄ vol.%	C ₂ H ₆ vol.%	C ₃ H ₆ vol.%	C ₃ H ₈ vol.%
2	0.53	650	22.9	47	22.1	5.3	5.5	10	55	4.8	0.31	1.1	0.28	0.52
2	0.53	700	22.1	44.7	22.1	6.6	6.2	22.5	37.6	4.4	0.29	0.98	0.26	0.49
2	0.53	750	20.6	43.5	25.3	7.6	7	36.5	24.2	3.4	0.21	0.75	0.2	0.37
2	0.53	800	18.6	42.3	27.7	8.4	7.1	44	19.6	3.1	0.22	0.68	0.19	0.34
2	0.53	850	17.8	40.7	30.8	9.3	7.3	51.6	20.5	3.1	0.25	0.66	0.18	0.33

T₁: Temperature of 1st reactor

Char g	Tar g	Gas g	Product gas volume ml	H ₂ ml	CO ml	CO ₂ ml	CH ₄ ml	C ₂ H ₄ ml	C ₂ H ₆ ml	C ₃ H ₆ ml	C ₃ H ₈ ml
0.58	1.19	0.56	484	26.7	48.2	261	22.9	1.5	5.3	1.3	2.5
0.56	1.13	0.56	565	36	142	196	24	1.6	5.3	1.4	2.6
0.52	1.1	0.64	705	50	257	168	24	1.47	5.2	1.4	2.5
0.47	1.07	0.7	775	54	341	150	24	1.6	5.3	1.5	2.6
0.45	1.03	0.78	775	56	400	157	24	1.94	5.2	1.38	2.5

Table C2 Effect of temperature during two-stage operation

MBM g	O₂ g	T₂ °C	T₁ °C	Char wt. %	Tar wt. %	Gas wt. %	Calorific value of product gas MJ/m³	H₂ vol.%	CO vol.%	CO₂ vol.%	CH₄ vol.%	C₂H₄ vol.%	C₂H₆ vol.%	C₃H₆ vol.%	C₃H₈ vol.%
2	0.53	650	850	17.8	26.5	42.3	18.1	7.4	41.6	21	9.46	8.3	1.5	2.9	0.24
2	0.53	700	850	17.4	24.9	43.1	17.8	8.8	40.4	23.8	9.44	7.8	1.5	2.76	0.25
2	0.53	750	850	17.8	22.1	44.7	17.7	9.9	38.5	20.7	10.68	8.7	1.19	2.04	0.12
2	0.53	800	850	17.4	19	50.2	16.4	14	36.1	20	11.6	8.3	0.7	0.7	0.02
2	0.53	850	850	17.8	17.4	52.2	16.1	21.2	36.2	19.7	10.2	7.7	0.52	0.41	0.008

T₂: Temperature of 2nd reactor

83

Char g	Tar g	Gas g	Product gas volume ml	H₂ ml	CO ml	CO₂ ml	CH₄ ml	C₂H₄ ml	C₂H₆ ml	C₃H₆ ml	C₃H₈ ml
0.45	0.67	1.06	984	72.3	409	202.4	91.5	81.4	14.8	28	2.3
0.45	0.63	1.09	980	86	393	230	92.2	77.3	14.7	26.2	2.4
0.45	0.56	1.2	1075	106.7	413.5	221	112.9	93.5	12.7	21.5	1.3
0.44	0.48	1.27	1300	181.4	468.6	258.3	148.4	108.5	8.8	8.8	0.21
0.45	0.44	1.3	1380	292.6	500.8	263.9	137.7	106.5	7.2	5.6	0.1

Table C3 Effect of equivalence ration in two-stage operation

MBM g	O ₂ g	ER	T ₂ °C	T ₁ °C	Char wt. %	Tar wt. %	Gas wt. %	Calorific value of product gas MJ/m ³	H ₂ vol. %	CO vol. %	CO ₂ vol. %	CH ₄ vol. %	C ₂ H ₄ vol. %	C ₂ H ₆ vol. %	C ₃ H ₆ vol. %	C ₃ H ₈ vol. %
2	0.4	0.15	850	850	20	19.6	43.3	16.61	17.3	32.9	16.8	11.6	8.9	0.61	0.55	0.01
2	0.53	0.2	850	850	17.8	17.4	52.2	16.05	21.2	36.2	19.7	10.2	7.7	0.52	0.41	0.008
2	0.67	0.25	850	850	16.1	16.1	54.7	15.75	18.8	37.4	22.1	9.9	7.56	0.55	0.45	0.01
2	0.81	0.3	850	850	14.2	14.6	56.2	15.04	16.9	36.5	24.4	9.4	7.26	0.51	0.46	0.01

Char g	Tar g	Gas g	Product gas volume ml	H ₂ ml	CO ml	CO ₂ ml	CH ₄ ml	C ₂ H ₄ ml	C ₂ H ₆ ml	C ₃ H ₆ ml	C ₃ H ₈ ml
0.48	0.47	1.04	1169	202	384	191	133	104	7.1	6.3	0.12
0.45	0.44	1.32	1380	292.6	500.8	263.9	137.7	106.5	7.2	5.6	0.1
0.43	0.43	1.46	1444	271	539	309	140	108	7.8	6.4	0.13
0.4	0.41	1.56	1535	259	560	362	141	111	7.9	6.9	0.13

Table C4 Effect of packed bed height during two-stage operation

MBM g	O ₂ g	Packing height mm	T ₂ °C	T ₁ °C	Char wt. %	Tar wt. %	Gas wt. %	Calorific value of product gas MJ/m ³	H ₂ vol.%	CO vol.%	CO ₂ vol.%	CH ₄ vol.%	C ₂ H ₄ vol.%	C ₂₊ Vol. %
2	0.53	40	850	850	17.4	18.6	50.6	16.17	18.9	39.3	19.7	10.7	7.59	0.835
2	0.53	60	850	850	17.8	17.4	52.1	16.05	21.2	36.2	19.7	10.2	7.7	0.938
2	0.53	80	850	850	17.8	16.6	52	16.33	21.7	37.6	19.6	9.8	7.69	1.194
2	0.53	100	850	850	17.4	14.2	54.6	16.54	22.3	40.7	19.2	10.3	7.47	0.825

Char g	Tar g	Gas g	Product gas volume ml	H ₂ ml	CO ml	CO ₂ ml	CH ₄ ml	C ₂ H ₄ ml	C ₂₊ ml
0.44	0.47	1.27	1300	245	510	249	136	98.6	10.8
0.45	0.44	1.32	1380	292.6	500.8	263.9	137.7	106.5	12.9
0.45	0.42	1.3	1350	292	508	257.8	130.3	103.8	16
0.44	0.36	1.37	1390	309.3	565.2	259.7	141.2	103.8	11.6

Table C5 Replicate runs of Phase I

Effect of temperature during single stage operation

MBM g	O ₂ g	T ₁ °C	Char wt. %	Tar wt. %	Gas wt. %	Calorific value of product gas MJ/m ³	H ₂ vol. %	CO vol. %	CO ₂ vol. %	CH ₄ vol. %	C ₂ H ₄ vol. %	C ₂ H ₆ vol. %	C ₃ H ₆ vol. %	C ₃ H ₈ vol. %
2	0.53	850	17.4	39.9	32	9.4	7	53.4	19.1	3	0.3	0.65	0.18	0.33

Char g	Tar g	Gas g	Product gas volume ml	H ₂ ml	CO ml	CO ₂ ml	CH ₄ ml	C ₂ H ₄ ml	C ₂ H ₆ ml	C ₃ H ₆ ml	C ₃ H ₈ ml
0.44	1.01	0.81	808	55.5	431	154	24	2.5	5.3	1.5	2.6

Effect of temperature during two-stage operation

MBM g	O ₂ g	T ₂ °C	T ₁ °C	Char wt. %	Tar wt. %	Gas wt. %	Calorific value of produc t gas MJ/m ³	H ₂ vol. %	CO vol. %	CO ₂ vol. %	CH ₄ vol. %	C ₂ H ₄ vol. %	C ₂ H ₆ vol. %	C ₃ H ₆ vol. %	C ₃ H ₈ vol. %
2	0.53	850	850	17.4	17.8	53.4	16.1	20.6	36.7	18.1	10.7	7.6	0.4	0.3	0.004

Char g	Tar g	Gas g	Produ ct gas volum e ml	H ₂ ml	CO ml	CO ₂ ml	CH ₄ ml	C ₂ H ₄ ml	C ₂ H ₆ ml	C ₃ H ₆ ml	C ₃ H ₈ ml
0.44	0.45	1.35	1450	297	528	263	154	110	5.7	4.2	0.006

Effect of equivalence ratio during two-stage operation

MBM g	O ₂ g	ER	T ₂ °C	T ₁ °C	Char wt. %	Tar wt. %	Gas wt. %	Calorific value of product gas MJ/m ³	H ₂ vol. %	CO vol. %	CO ₂ vol. %	CH ₄ vol. %	C ₂ H ₄ vol. %	C ₂ H ₆ vol. %	C ₃ H ₆ vol. %	C ₃ H ₈ vol. %
2	0.53	0.2	850	850	17.4	17.8	53.4	16.1	20.6	36.7	18.1	10.7	7.6	0.4	0.3	0.004

Char g	Tar g	Gas g	Product gas volume ml	H ₂ ml	CO ml	CO ₂ ml	CH ₄ ml	C ₂ H ₄ ml	C ₂ H ₆ ml	C ₃ H ₆ ml	C ₃ H ₈ ml
0.44	0.45	1.35	1450	297	528	263	154	110	5.7	4.2	0.006

Effect of packed bed height during two-stage operation

MBM g	O ₂ g	Packing height mm	T ₂ °C	T ₁ °C	Char wt. %	Tar wt. %	Gas wt. %	Calorific value of product gas MJ/m ³	H ₂ vol. %	CO vol. %	CO ₂ vol. %	CH ₄ vol. %	C ₂ H ₄ vol. %	C ₂₊ Vol. %
2	0.53	100	850	850	17.8	14.6	55.3	16.2	22.4	39.4	19.3	10	7.3	0.85

Char g	Tar g	Gas g	Product gas volume ml	H ₂ ml	CO ml	CO ₂ ml	CH ₄ ml	C ₂ H ₄ ml	C ₂₊ ml
0.45	0.37	1.4	1420	317	560	274	143	103	12

Phase II: Gasification of MBM using steam in single stage and two-stage operations

Table C6 Effect of temperature during single stage operation

MBM g	Steam g	T₁ °C	Char wt. %	Liquid wt. %	Gas wt. %	Calorific value of product gas MJ/m³	H₂ vol.%	CO vol.%	CO₂ vol.%	CH₄ vol.%	C₂H₄ vol.%	C₂₊ vol.%
2	0.99	650	21.7	57.9	8.7	11.24	42	10.2	25.9	7	0.42	2.65
2	0.99	700	18.7	55.5	9.7	10.74	45.7	14.2	20.6	5	0.3	1.92
2	0.99	750	17.73	54.5	10.4	11	46.9	19.7	17.1	4.5	0.3	1.59
2	0.99	800	15.4	53.9	15.1	10.7	50.4	21.5	14.4	3.21	0.17	1.06
2	0.99	850	14.1	52.2	18.1	11.5	52.2	26.8	12.8	3.12	0.16	1.02

T₁: Temperature of 1st reactor

Char g	Liquid g	Gas g	Product gas volume ml	H₂ ml	CO ml	CO₂ ml	CH₄ ml	C₂H₄ ml	C₂₊ ml
0.65	1.73	0.26	350	147	35.5	90.8	24.6	1.5	9.3
0.56	1.66	0.29	440	201	62	90.5	22	1.3	8.2
0.53	1.63	0.31	480	225	94	82	21	1.2	7.6
0.46	1.61	0.47	785	395	168	113	25	1.3	8.2
0.42	1.56	0.54	844	440	226	108	26	1.3	8.2

Table C7 Effect of temperature during two-stage operation

MBM g	Steam g	T₂ °C	T₁ °C	Char wt. %	Liquid wt. %	Gas wt. %	Calorific value of product gas MJ/m³	H₂ vol.%	CO vol.%	CO₂ vol.%	CH₄ vol.%	C₂H₄ vol.%	C₂₊ vol.%
2	0.99	650	850	15.1	39.1	26.8	16.8	39.9	23.6	10.5	7.8	5.1	4.2
2	0.99	700	850	15.4	38.5	27.8	18.8	38.2	23.9	9.5	10.2	7.7	3.63
2	0.99	750	850	15.4	35.5	29.8	17.83	39.7	23.1	9.5	11.4	7.9	1.602
2	0.99	800	850	15.4	33.4	31.4	18	40.8	23.8	9.5	12.5	8.15	0.837
2	0.99	850	850	15.4	32.4	32.1	17.5	46.2	23.9	9.8	14.2	5.9	0.29

68

T₂: Temperature of 2nd reactor

Char g	Liquid g	Gas g	Product gas volume ml	H₂ ml	CO ml	CO₂ ml	CH₄ ml	C₂H₄ ml	C₂₊ ml
0.45	1.17	0.8	1160	463	273	121	90	58	46
0.46	1.15	0.83	1175	448	280	111	119	90	42.4
0.46	1.06	0.89	1315	522	304	124	150	104	20.2
0.46	1	0.94	1367	558	326	130	170	111	11.4
0.46	0.97	0.96	1420	655	337.8	139	200.7	85.5	4.1

Table C8 Effect of steam/MBM during two-stage operation

MBM g	Steam g	S/B	T ₂ °C	T ₁ °C	Char wt. %	Liquid wt. %	Gas wt. %	Calorific value of product gas MJ/m ³	H ₂ vol.%	CO vol.%	CO ₂ vol.%	CH ₄ vol.%	C ₂ H ₄ vol.%	C ₂₊ vol.%
2	0.33	0.2	850	850	27	29.2	23.6	21	36.2	19.6	7.9	23.2	8.7	0.42
2	0.66	0.4	850	850	19.9	32.7	27.4	18.3	43.6	22.8	7.3	17.6	5.8	0.28
2	0.99	0.6	850	850	15.4	32.4	31.9	17.6	46.2	23.8	9.8	14.2	6.1	0.29
2	1.32	0.8	850	850	13	36.7	30	17.6	47.1	23.3	9.2	14.5	5.3	0.28

Char g	Liquid g	Gas g	Product gas volume ml	H ₂ ml	CO ml	CO ₂ ml	CH ₄ ml	C ₂ H ₄ ml	C ₂₊ ml
0.63	0.68	0.55	815	295	159.5	63.3	189	71.1	3.3
0.53	0.87	0.73	1145	500	261.6	82.8	201.6	65.9	3
0.46	0.97	0.96	1420	655	337.8	139	200.7	85.5	4.1
0.43	1.22	0.99	1510	710	352	137.7	220.3	80.6	4.4

Table C9 Effect of packed bed height during two-stage operation

MBM g	Steam g	Packing height mm	T₂ °C	T₁ °C	Char wt. %	Liquid wt. %	Gas wt. %	Calorific value of product gas MJ/m³	H₂ vol.%	CO vol.%	CO₂ vol.%	CH₄ vol.%	C₂₊ vol.%
2	1.32	40	850	850	13	38.6	29.5	17.4	45	22.5	12.4	14.5	6.3
2	1.32	60	850	850	13	36.7	30	17.6	47.1	23.3	9.2	14.5	5.58
2	32	80	850	850	13	35.6	30.1	17.2	48.2	22	10.6	13.5	6
2	1.32	100	850	850	13	34.9	31.6	17.4	48.9	22.7	10.4	13.3	6.1

Char g	Liquid g	Gas g	Product gas volume ml	H₂ ml	CO ml	CO₂ ml	CH₄ ml	C₂₊ ml
0.43	1.28	0.98	1395	628.8	313.9	172.4	202	87.6
0.43	1.22	0.99	1510	710	352	137.7	220	85
0.43	1.18	1	1555	749.5	342.3	164.9	210.7	93.4
0.43	1.16	1.05	1575	769.7	357.1	163.2	209.5	96.7

Table C10 Replicate runs of Phase II

Effect of temperature during single stage operation

MBM g	Steam g	T ₁ °C	Char wt. %	Liquid wt. %	Gas wt. %	Calorific value of product gas MJ/m ³	H ₂ vol. %	CO vol. %	CO ₂ vol. %	CH ₄ vol. %	C ₂ H ₄ vol. %	C ₂₊ vol. %
2	0.99	850	14.38	51.2	18.7	11.4	52.8	25.1	12.6	3.1	0.2	0.95
			Char g	Liquid g	Gas g	Product gas volume ml	H ₂ ml	CO ml	CO ₂ ml	CH ₄ ml	C ₂ H ₄ ml	C ₂₊ ml
			0.43	1.53	0.57	923	487	231.7	116.5	29	1.8	8.8

Effect of temperature during two-stage operation

MBM g	Steam g	T ₂ °C	T ₁ °C	Char wt. %	Liquid wt. %	Gas wt. %	Calorific value of product gas MJ/m ³	H ₂ vol. %	CO vol. %	CO ₂ vol. %	CH ₄ vol. %	C ₂ H ₄ vol. %	C ₂₊ vol. %
2	0.99	850	850	15.1	33.1	31.8	17.5	47.1	22.7	9.4	15	5.4	0.25
				Char g	Liquid g	Gas g	Product gas volume ml	H ₂ ml	CO ml	CO ₂ ml	CH ₄ ml	C ₂ H ₄ ml	C ₂₊ ml
				0.45	0.99	0.95	1450	684	329	136.5	217.8	78.5	3.6

Effect of steam/MBM during two-stage operation

MBM g	Steam g	S/B	T ₂ °C	T ₁ °C	Char wt. %	Liquid wt. %	Gas wt. %	Calorific value of product gas MJ/m ³	H ₂ vol.%	CO vol.%	CO ₂ vol.%	CH ₄ vol.%	C ₂ H ₄ vol.%	C ₂₊ vol.%
2	1.32	0.8	850	850	13	36.7	30.1	17.6	49.2	22.9	9.6	15.1	5	0.25

Char g	Liquid g	Gas g	Product gas volume ml	H ₂ ml	CO ml	CO ₂ ml	CH ₄ ml	C ₂ H ₄ ml	C ₂₊ ml
0.43	1.22	1	1535	756	351	146	232.8	76.4	3.8

Effect of packed bed height during two-stage operation

MBM g	Steam g	Packing height mm	T ₂ °C	T ₁ °C	Char wt. %	Liquid wt. %	Gas wt. %	Calorific value of product gas MJ/m ³	H ₂ vol.%	CO vol.%	CO ₂ vol.%	CH ₄ vol.%	C ₂₊ vol.%
2	1.32	100	850	850	13	35.2	30.4	16.7	47.2	21.7	10.8	12.7	6.1

Char g	Liquid g	Gas g	Product gas volume ml	H ₂ ml	CO ml	CO ₂ ml	CH ₄ ml	C ₂₊ ml
0.43	1.17	1	1520	715	327	166	191	92.5

APPENDIX D: Permission for figures, and tables

D1: Letter of permission for Fig. 2.1

Date: **Wed, 05 Aug 2009 09:54:29 -0400**

From: "[Macintyre, Stacy](mailto:Stacy.Macintyre@eia.doe.gov)" <Stacy.Macintyre@eia.doe.gov> [Block Address](#)

To: "[Chirayu Soni](mailto:chs332@mail.usask.ca)" <chs332@mail.usask.ca>

Subject: **RE: Permission to use Fig. 10 in International Energy Outlook May 2009**

Dear Chirayu Soni,

Thank you for your request to use an image from the International Energy Outlook. U.S. Government publications are in the public domain and are not subject to copyright protection. You may use and/or distribute any of our data, files, databases, reports, graphs, charts, and other information products that are on our website or that you receive through our email distribution service. However, if you use or reproduce any of our information products, you should use an acknowledgment, which includes the publication date, such as: "Source: Energy Information Administration (Oct 2008)."

Regards,

Stacy MacIntyre

National Energy Information Center

Energy Information Administration/U.S. Dept. of Energy

From: Chirayu Soni [mailto:chs332@mail.usask.ca]

Sent: Tuesday, August 04, 2009 4:20 PM

To: Macintyre, Stacy

Subject: Permission to use Fig. 10 in International Energy Outlook May 2009

Hello,

My name is Chirayu Soni and I'm a chemical engineering master's student at the University of Saskatchewan in Canada. I would like to have your permission to use your Fig. 10 World marketed energy consumption, 1980-2030 (Chapter 1, International Energy Outlook May 2009) in the introductory material for my thesis.

My thesis is on Gasification of Meat and Bone. Basically, gasification is a well known process for producing syngas. The syngas could be used for generating electricity or in other applications. I would like to use this figure to explain the world energy consumption now and in the future.

Thank you,

Sincerely,

Chirayu Soni

D2 Permission for Fig. 2.2

License Number 2242071155701

License date Aug 04, 2009

Licensed content publisher Elsevier

Licensed content publication

Renewable and Sustainable Energy Reviews

Licensed content title

The reduction and control technology of tar during biomass gasification/pyrolysis: An overview

Licensed content author Jun Han and Heejoon Kim

Licensed content date February 2008

Volume number 12

Issue number 2

Pages 20

Type of Use Thesis / Dissertation

Portion Figures/table/illustration/abstracts

Portion Quantity 1

Format Both print and electronic

You are the author of this Elsevier article No

Are you translating? No

Order Reference Number

Expected publication date Sep 2009

Elsevier VAT number GB 494 6272 12

Billing type Invoice

Company Chirayu G Soni

Billing address Dept of Chemical Eng.,

57 Campus Dr, University of Saskatchewan Saskatoon, SK S7N5A9 Canada

Customer reference info

Permissions price 0.00 USD

Value added tax 0.0% 0.00 USD

Total 0.00 USD

D3: Permission for Fig. 2.3

License Number 2242080221295

License date Aug 04, 2009

Licensed content publisher Elsevier

Licensed content publication Energy Policy

Licensed content title: Atmospheric stabilization of CO₂ emissions: Near-term reductions and absolute versus intensity-based targets

Licensed content author Govinda R. Timilsina

Licensed content date June 2008

Volume number 36

Issue number 6

Pages 10

Type of Use Thesis / Dissertation

Portion Figures/table/illustration/abstracts

Portion Quantity 1

Format Both print and electronic

You are the author of this Elsevier article No

Are you translating? No

Order Reference Number

Expected publication date Sep 2009

Elsevier VAT number GB 494 6272 12

Billing type Invoice

Company Chirayu G Soni

Billing address Dept of Chemical Eng., 57 Campus Dr, University of Saskatchewan

Saskatoon, SK S7N5A9 Canada

Customer reference info

Permissions price 0.00 USD

Value added tax 0.0% 0.00 USD

Total 0.00 USD

D4: Permission for Table 2.2

License Number 2242080622873

License date Aug 04, 2009

Licensed content publisher Elsevier

Licensed content publication Biomass and Bioenergy

Licensed content title Electricity from biomass in the European Union—With or without biomass import

Licensed content author Klaus Skytte, Peter Meibom and Thomas Capral Henriksen

Licensed content date May 2006

Volume number 30

Issue number 5

Pages 8

Type of Use Thesis / Dissertation

Portion Figures/table/illustration/abstracts

Portion Quantity 1

Format Both print and electronic

You are the author of this Elsevier article No

Are you translating? No

Order Reference Number

Expected publication date Sep 2009

Elsevier VAT number GB 494 6272 12

Billing type Invoice

Company Chirayu G Soni

Billing address Dept of Chemical Eng., 57 Campus Dr, University of Saskatchewan

Saskatoon, SK S7N5A9 Canada

Customer reference info

Permissions price 0.00 USD

Value added tax 0.0% 0.00 USD

Total 0.00 USD